N-terminal regions of Mps1 kinase determine functional bifurcation

Yasuhiro Araki,[1] Linda Gombos,[1] Suellen P.S. Migueleti,[1] Lavanya Sivashanmugam,[1] Claude Antony,[2] and Elmar Schiebel[1]

[1]Zentrum für Molekulare Biologie der Universität Heidelberg (ZMBH), Deutsches Krebsforschungszentrum–ZMBH Allianz, 69120 Heidelberg, Germany
[2]European Molecular Biology Laboratory, 69117 Heidelberg, Germany

Mps1 is a conserved kinase that in budding yeast functions in duplication of the spindle pole body (SPB), spindle checkpoint activation, and kinetochore biorientation. The identity of Mps1 targets and the subdomains that convey specificity remain largely unexplored. Using a novel combination of systematic deletion analysis and chemical biology, we identified two regions within the N terminus of Mps1 that are essential for either SPB duplication or kinetochore biorientation. Suppression analysis of the *MPS1* mutants defective in SPB duplication and biochemical enrichment of Mps1 identified the essential SPB components Spc29 and the yeast centrin Cdc31 as Mps1 targets in SPB duplication. Our data suggest that phosphorylation of Spc29 by Mps1 in G1/S recruits the Mps2–Bbp1 complex to the newly formed SPB to facilitate its insertion into the nuclear envelope. Mps1 phosphorylation of Cdc31 at the conserved T110 residue controls substrate binding to Kar1 protein. These findings explain the multiple SPB duplication defects of *mps1* mutants on a molecular level.

Introduction

The spindle pole body (SPB), the functional equivalent of the mammalian centrosome, provides microtubule (MT)-organizing functions in budding yeast (Jaspersen and Winey, 2004). The SPB is embedded in the nuclear envelope (NE) in a similar way to the nuclear pore complex (Jaspersen and Winey, 2004). This embedding allows the SPB to simultaneously organize both the cytoplasmic and nuclear MTs that execute essential functions in nuclear positioning and chromosome segregation, respectively.

The yeast SPB duplicates once per cell cycle (Adams and Kilmartin, 2000). SPB duplication is a cell cycle–regulated process that starts in G1 phase of the cell cycle with the extension of an SPB substructure named the half bridge. The satellite then develops on the cytoplasmic face of the NE at the distal end of the elongated half bridge (Adams and Kilmartin, 1999; Kilmartin, 2003). After the start of the cell cycle, the satellite expands into a duplication plaque that becomes inserted into the NE followed by the assembly of the nuclear side of the SPB (Byers and Goetsch, 1975; Winey et al., 1991, 1993; Kilmartin and Goh, 1996; Sundberg et al., 1996; Adams and Kilmartin, 1999).

Correspondence to Elmar Schiebel: e.schiebel@zmbh.uni-heidelberg.de

Abbreviations used in this paper: 5-FOA, 5-fluoroorotic acid; CBB, Coomassie brilliant blue; CEN, centromere; LC, liquid chromatography; MBP, myelin basic protein; MS, mass spectrometry; MT, microtubule; NE, nuclear envelope; SAC, spindle assembly checkpoint; SPB, spindle pole body; TAP, tandem affinity purification.

SPB duplication is regulated through phosphorylation. Cdk1 and Mps1 kinase are mainly responsible for this regulation (Lauzé et al., 1995; Ubersax et al., 2003; Loog and Morgan, 2005). Cdk1 either inhibits or promotes SPB duplication, depending on which phase of the cell cycle it is acting in (Haase et al., 2001). In G1 phase, Cdk1 promotes SPB duplication through phosphorylation of Mps1 and the SPB component Spc42 (Jaspersen et al., 2004). Recently, it was shown that Mps1 kinase phosphorylates the SPB component Spc29 at T240. The T240A mutation of Spc29 leads to instability of the protein (Holinger et al., 2009). It is currently unclear whether this is the only phosphorylation event executed by Mps1 to drive SPB duplication.

Jones et al. (2005) constructed the *mps1-as1* mutant, which is specifically inhibited in its kinase activity by the ATP analogue 1NM-PP1. Addition of 1NM-PP1 to *mps1-as1* cells in G1 disrupted SPB duplication and the spindle assembly checkpoint (SAC). In contrast, poisoning *mps1-as1* cells later, when cells have already duplicated their SPBs, leads to failure of sister kinetochore biorientation (Jones et al., 2005; Maure et al., 2007). Targets of Msp1 at kinetochores are Ndc80 and the DASH complex. Mps1-dependent phosphorylation of Ndc80 is important for SAC

The Rockefeller University Press $30.00
J. Cell Biol. Vol. 189 No. 1 41–56
www.jcb.org/cgi/doi/10.1083/jcb.200910027

activation at kinetochores (Kemmler et al., 2009). Phosphorylation of the DASH complex component Dam1 by Mps1 couples efficient binding of kinetochores to MT plus ends (Shimogawa et al., 2006).

In this study, we used a novel combination of deletion analysis and chemical genetics to study the function of the N-terminal nonkinase domain of Mps1. This analysis identified distinct regions within the N terminus of Mps1 with specific functions in SPB duplication and kinetochore biorientation. Using a novel *mps1* mutant allele that was defective in SPB duplication but not kinetochore biorientation, we identified the Mps2–Bbp1–Spc29 SPB membrane insertion machinery (Elliott et al., 1999; Muñoz-Centeno et al., 1999; Schramm et al., 2000) as a critical target of Mps1. An additional substrate of Mps1 at the SPB is the yeast centrin Cdc31 (Baum et al., 1986; Spang et al., 1993). Our data indicate that phosphorylation of Cdc31 regulates its binding to the essential half bridge protein Kar1 (Rose and Fink, 1987; Spang et al., 1995).

Results

N-terminal regions of Mps1 are essential for viability

As a starting model, we assumed that regions in the N-terminal nonkinase domain of Mps1 are instrumental in conferring target specificity to the kinase. To test this idea, we introduced small deletions of 50 codons within the N- and C-terminal nonkinase domains of *MPS1* and transformed the *mps1* alleles in the *MPS1* shuffle strain YAY406 (Fig. 1 A). Transformants were tested for growth on plates in which the inclusion of 5-fluoroorotic acid (5-FOA) selected against the centromere (CEN)-*MPS1 URA3*-based plasmid of strain YAY406 so that the *mps1* allele became the sole source of Mps1 activity. Some deletion mutants were viable on 5-FOA plates (Fig. 1 B, rows 3, 4, 8, and 9), whereas others did not fulfill essential *MPS1* functions (Fig. 1 B, rows 2, 5–7, and 10–12). Most of the nonfunctional *mps1* alleles were expressed in yeast, were able to dimerize with wild-type Mps1 (Fig. S1 A), and had kinase activity (Fig. 1 C). The $mps1^{\Delta 151–200}$ (*mps1-A*), $mps1^{\Delta 201–250}$ (*mps1-B*), and $mps1^{\Delta 251–300}$ (*mps1-C*) constructs were particularly interesting because they did not support the growth of yeast cells, even though the specific kinase activity of the encoded mps1-A, -B, and -C proteins was comparable with, or even higher than, that of wild-type Mps1 (Fig. 1 C). This suggests that the mps1-A, -B, and -C proteins are unable to execute at least one essential function of Mps1.

Intergenetic complementation of *MPS1* deletion mutants

The N-terminal Mps1 deletion constructs may fail to function in vivo because the deleted region enables the kinase to perform an essential function in SPB duplication, kinetochore biorientation, or both. The combination of two deletion constructs may restore viability of cells if both *mps1* alleles together fulfill all essential functions of *MPS1*. Combining *mps1* deletion constructs in the yeast *MPS1* shuffle strain tested this possibility. *mps1-A* combined with either *mps1-B* or *-C* (all chromosomally integrated) supported cell growth on 5-FOA plates (Fig. 2 A, rows 9 and 10). The combined *mps1-A mps1-B* or *mps1-A mps1-C* were expressed similarly (Fig. S1 B) and mps1-A–TAP (tandem affinity purification) coimmunoprecipitated with mps1-B–6HA and mps1-C–6HA (Fig. S1 C), suggesting the formation of mps1-A/-B and mps1-A/-C complexes. Importantly, integration of two copies of *mps1-A* (Fig. 2 A, row 4), *-B* (row 5), or *-C* (row 6) did not allow growth on 5-FOA plates. Thus, it is not the increase in Mps1 kinase activity that restores viability of the combined *mps1-A*, *-B*, or *-C* deletion mutants. Rather, *mps1-A mps1-B* and *mps1-A mps1-C* cells probably now survive because of complementation of essential functions: one set being executed by the one allele while the other allele performs another set.

In contrast to *mps1-A*, *-B*, and *-C*, the gene products of $mps1^{\Delta 4–50}$ and $mps1^{\Delta 716–764}$ had reduced specific kinase activity (Fig. 1 C), and two copies of each allele restored viability (Fig. 2 A, rows 3 and 8). This result is consistent with the idea that aa 4–50 and 716–764 are important for full kinase activity. However, our analysis does not exclude the possibility that aa 4–50 and 716–764 of Mps1 may fulfill additional functions such as in localization of the protein.

The defects of the *mps1-A*, *-B*, and *-C* cell alleles were analyzed using a novel strategy. We combined two complementing *mps1* deletion alleles, one of which carried an as1 mutation in its kinase domain (Bishop et al., 2000; Jones et al., 2005). 1NM-PP1 competes with ATP for binding to the active site of mps1-as1, whereas the unmodified Mps1 kinase remains unaffected. *mps1-A–as1 mps1-B* cells were viable under normal growth conditions but failed to grow when the kinase activity of mps1-A–as1 was inhibited by 1NM-PP1. Similar observations were made with other *mps1-as1 mps1* combinations (Fig. 2 B).

If our hypothesis of the complementation of essential functions were correct, we would expect distinct phenotypes depending on which of the two *mps1* alleles was inhibited. Addition of 1NM-PP1 should inactivate mps1-A–as1 and therefore reveal the phenotype of the *mps1-B* allele. To test this, we first compared the flow cytometry profiles of α-factor–synchronized *mps1-A–as1 mps1-B* cells with *mps1-A mps1-B–as1* cells after incubation with 1NM-PP1 (Fig. 2 C). In the presence of 1NM-PP1, *mps1-A–as1 mps1-B* cells replicated the DNA (2C peak after ∼90 min) and then showed strong genetic instability giving rise to >2C and <1C DNA peaks. This phenotype is similar to that of *mps1-as1* cells, which have defects in both SPB duplication and SAC function (Winey et al., 1991; Dorer et al., 2005). In contrast, the presence of 1NM-PP1 did not grossly affect the flow cytometry profile of *mps1-A mps1-B–as1* cells (Fig. 2 C).

A comparison between synchronized *mps1-A–as1 mps1-C* cells and *mps1-A mps1-C–as1* cells incubated with 1NM-PP1 revealed that the first cell type replicated the DNA and became aneuploid soon after this (120 min; Fig. 2 C), whereas *mps1-A mps1-C–as1* cells duplicated the chromosomes (t = 60) followed by only a modest degree of genetic instability (Fig. 2 C). This analysis validates our approach and indicates that deletions within essential regions in the N terminus of *MPS1* cause different phenotypes.

aa 151–200 of Mps1 function in kinetochore biorientation, and aa 201–300 function in SPB duplication

We asked whether *mps1-as1 mps1* cells are defective in SPB duplication. The addition of 1NM-PP1 to *mps1-A–as1 mps1-B*

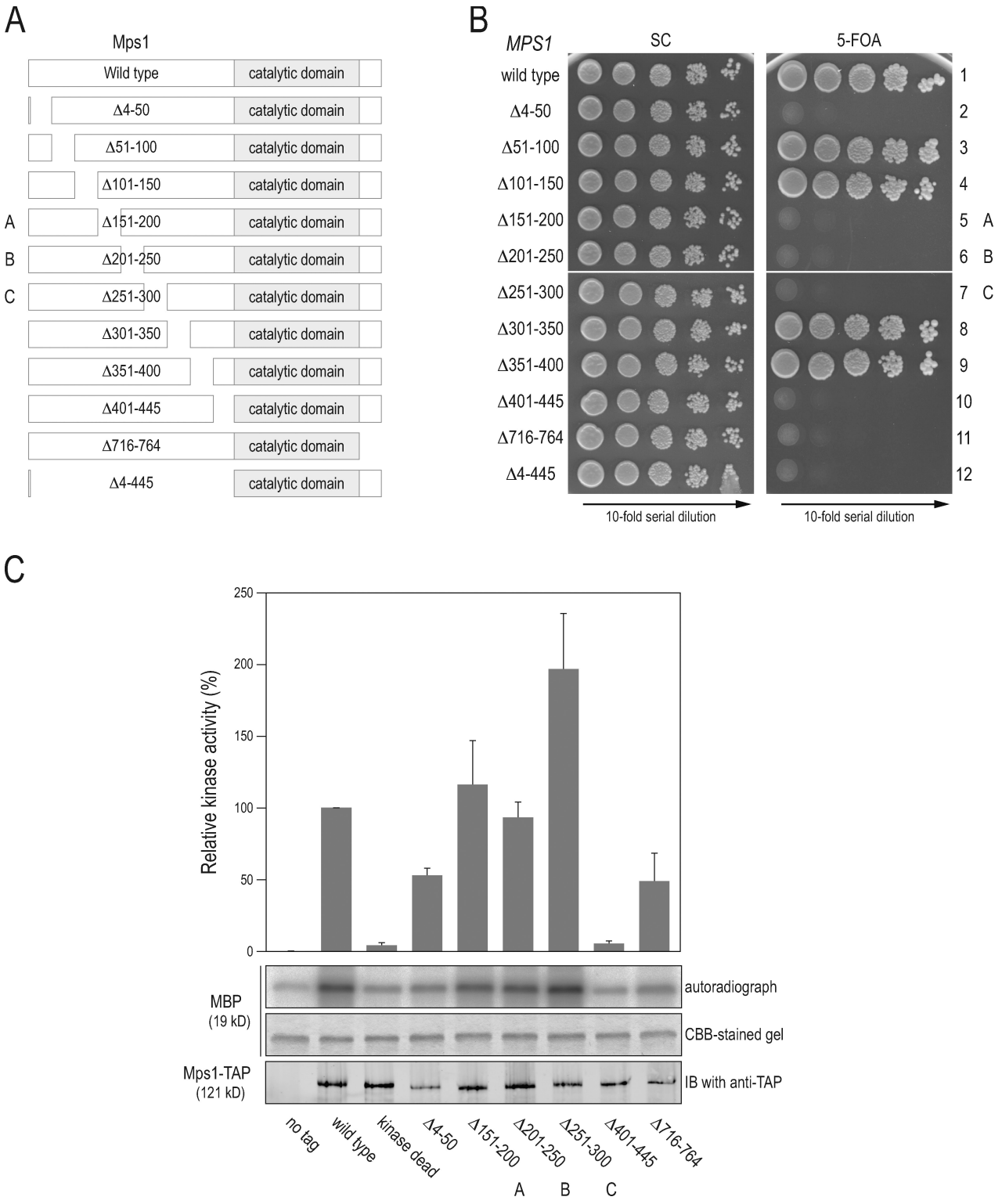

Figure 1. **Nonkinase regions of Mps1 are essential for viability.** (A) Deletions in the nonkinase N- and C-terminal regions of Mps1 were introduced as outlined. (B) YAY406 cells with the indicated plasmids encoding *mps1* mutant alleles were grown at 23°C for 3 d on synthetic complete (SC) and 5-FOA plates. (C) Specific kinase activity of Mps1 constructs. TAP-tagged Mps1 (lane 2, wild type), kinase-dead mps1^{D580A} (lane 3), and mps1 deletion mutants (lanes 4–9) were purified, and in vitro kinase assays were performed with MBP as substrate. The specific kinase activity as relative units is shown. MBP was detected by CBB and mps1 constructs by anti-TAP immunoblotting (IB). Error bars indicate SD.

or *mps1-A–as1 mps1-C* cells led to defects in mitotic spindle assembly (Fig. 3, A and B). About 50% of cells had monopolar spindles that were organized by only one SPB (Fig. 3, A and B [i]), whereas the remainder showed a monopolar spindle alongside a dead SPB, as characterized by a red Spc42-eqFP dot (Spc42 marks the central SPB layer; Donaldson and Kilmartin, 1996)

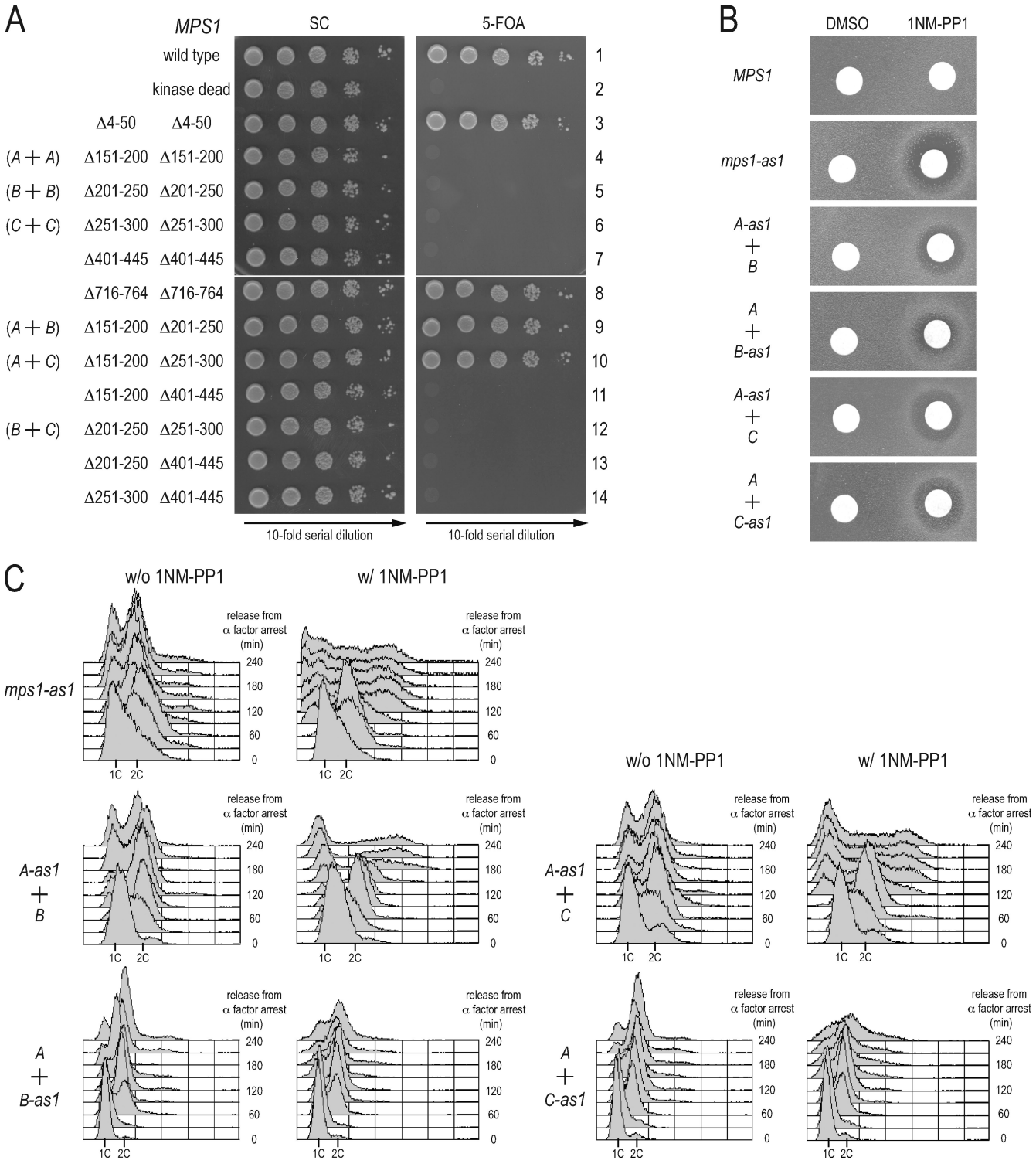

Figure 2. **Intergenetic complementation of *mps1* deletion mutants.** (A) Intergenetic complementation of *mps1* deletion mutants. *MPS1*, *mps1KD*, and the indicated *mps1* deletion constructs were integrated into the genome of the *MPS1* shuffle strain YAY406 (*mps1Δ* CEN-*URA3*-*MPS1*). Serial dilutions of cells were tested for growth at 23°C for 3 d. SC, synthetic complete. (B) Cells expressing the indicated *mps1* deletion alleles were uniformly plated onto YPD plates. Filters with 10 μM 1NM-PP1 or only DMSO were placed on top. Plates were incubated at 23°C for 2 d. (C) Flow cytometry analysis of *mps1* cells with (w/) or without (w/o) 1NM-PP1. Cells were synchronized with α-factor in G1 at 23°C followed by the release and the addition of 1NM-PP1.

that lacked a green nuclear GFP-tubulin signal (Fig. 3, A and B [ii, arrowhead]). The appearance of a dead SPB is characteristic for mutants with defects in duplication plaque insertion. Therefore, in these mutants, the newly formed SPB is unable to organize nuclear MTs (Winey et al., 1991). Importantly, *mps1-A–as1 mps1-B–as1* and *mps1-A–as1 mps1-C–as1* cells showed the same SPB defect as *mps1-as1* cells (Fig. S2 A), suggesting that 1NM-PP1 efficiently blocks kinase activity

of combined *mps1-as1 mps1* alleles. In contrast, most *mps1-A mps1-B–as1* and *mps1-A mps1-C–as1* cells duplicated their SPBs normally, as indicated by the formation of a bipolar spindle (Fig. 3, A and B [iii]). This analysis demonstrates that aa 201–300 of Mps1 are required for the kinase to promote SPB duplication, whereas aa 151–200 of Mps1 are not important for SPB duplication.

Next, we analyzed *mps1-A mps1-B–as1* and *mps1-A mps1-C–as1* cells for kinetochore segregation defects with an assay in which the *URA3* locus on chromosome V was marked by binding of Tet repressor–GFP to multiple tandem Tet operators (Michaelis et al., 1997). Whereas >95% of *MPS1* anaphase cells achieved successful biorientation of GFP-marked chromosome V (*URA3*-GFP) in the presence of 1NM-PP1, this number dropped to 78% in *mps1-A mps1-B–as1* cells and to 25% in *mps1-A mps1-C–as1* cells (Fig. 3 C). In the 22%/75% of monooriented *mps1-A mps1-B–as1* or *mps1-A mps1-C–as1* cells, respectively, about half of the sister kinetochores were associated with the SPB in the mother cell and the other half with the SPB in the daughter (Fig. 3 D, ii and iii). This random distribution contrasts with mutants of the aurora B complex and *mps1-as1* that show preferential association of sister kinetochores with the SPB in the daughter (Tanaka et al., 2002; Maure et al., 2007). One way to explain this difference is the disturbance of SPB inheritance in *mps1-A mps1-C–as1* cells (Pereira et al., 2001). However, the newly assembled SPB of *mps1-A mps1-C–as1* cells, as indicated by the weaker Spc42-eqFP signal, was still inherited preferentially to the mother cell (Fig. 3 E). Thus, aa 151–200 of Mps1 function in kinetochore biorientation.

mps1-as1 cells that have already duplicated the SPB show defects in kinetochore biorientation upon the subsequent addition of the inhibitor 1NM-PP1 (Maure et al., 2007). Thus, *mps1-A–as1 mps1-C* cells could be defective in kinetochore biorientation, but the phenotype is being masked by the failure in SPB duplication. To bypass the SPB duplication defect, we incubated α-factor–synchronized *mps1-as1*, *mps1-A–as1 mps1-C*, and *mps1-A mps1-C–as1* cells with 1NM-PP1 at different time points after the G1 release. The addition of 1NM-PP1 45, 60, or 75 min after release from the G1 block to *mps1-A–as1 mps1-C* cells allowed formation of bipolar spindles (addition at t = 0 caused mainly monopolar spindles and a dead pole). In the t = 45–75 min cells, most sister chromatids segregated in a bipolar fashion. Cells with anaphase spindles and monopolar orientation of *URA3*-GFP were rarely observed (Fig. 3 F). In contrast, *mps1-as1* and *mps1-A mps1-C–as1* cells grown under identical conditions exhibited defects in sister kinetochore biorientation (Fig. 3, F and G). Thus, *mps1-A–as1 mps1-C* cells are defective in SPB duplication but are fully competent to execute Mps1's function in kinetochore biorientation.

Finally, we analyzed the role of the N terminus of Mps1 in the SAC. *mps1* deletion mutants were incubated with the MT-depolymerizing drug nocodazole to trigger a SAC response. Wild-type *MPS1* and SAC-deficient *mad2Δ* cells were used as controls for cells with a functional and defective SAC, respectively. *mps1-A–as1 mps1-B*, *mps1-A mps1-B–as1*, *mps1-A–as1 mps1-C*, and *mps1-A mps1-C–as1* cells were all SAC deficient in the presence of the inhibitor 1NM-PP1 because they behaved as *mad2Δ* cells in the flow cytometry analysis (Fig. S1 D). A rather large portion of the N terminus of Mps1 is essential for SAC function.

Mps1 phosphorylates the SPB component Spc29 in G1/S

In our strain background, all *mps1-as1* alleles were sensitive for growth at elevated temperatures (Fig. S2 B). *mps1-as1*, *mps1-A–as1 mps1-B*, and *mps1-A–as1 mps1-C* cells failed to duplicate their SPBs at 37°C because of the malfunction of the *mps1-as1* allele (Fig. S2 C). In contrast, *mps1-A mps1-B–as1* or *mps1-A mps1-C–as1* cells grown at 37°C without 1NM-PP1 or at 23°C with 1NM-PP1 showed defects in kinetochore biorientation but not SPB duplication (Fig. 3 C, Fig. S2 C, and not depicted). Thus, the phenotypes of *mps1-as1 mps1* cells at 23°C with 1NM-PP1 and at 37°C without 1NM-PP1 are similar.

We used the failure of *mps1-A–as1 mps1-B* and *mps1-A–as1 mps1-C* cells to grow at 37°C for suppression analysis. *mps1-A–as1 mps1-B* and *mps1-A–as1 mps1-C* cells with high gene dosage of *MPS2*, *NBP1*, and *SPC29* were able to grow efficiently at 37°C (Fig. 4 A and not depicted). *SPC110* and *BBP1* were weak suppressors of the growth defect. In contrast, *MPS2*, *NBP1*, and *SPC29* did not suppress the growth defect of *mps1-as1* and *mps1-A mps1-C–as1* cells at 37°C (unpublished data). These data suggest that Mps1 regulates SPB duplication at the level of the Mps2–Bbp1–Nbp1 complex, which interacts with Spc29. *MPS2*, *BBP1*, and *NBP1* code for interacting proteins that are essential for the insertion of the newly assembled SPB into the NE (Winey et al., 1991; Elliott et al., 1999; Muñoz-Centeno et al., 1999; Schramm et al., 2000; Araki et al., 2006).

Because *SPC29* was the most efficient suppressor of the *mps1-A–as1 mps1-C* cells (Fig. 4 A), we focused our analysis on the regulation of Spc29 by Mps1. Analysis of α-factor–synchronized *SPC29-Flag* cells grown at 23°C showed a moderate but reproducible upshift of Spc29 in the SDS-PAGE gel when cells were in G1/S 60 min after the release of the cell cycle block (Fig. 4 B). Incubation of immunoprecipitated Spc29-Flag from synchronized cells of the 60-min time point (Fig. 4 B) with λ phosphatase led to the collapse of the slower-migrating Spc29 species into a single, faster-migrating protein band (Fig. 4 C). Thus, the mobility shift was caused by phosphorylation of the Spc29 protein. Phosphorylation was dependent on Mps1 activity because the reduced mobility of Spc29 was abolished when *mps1-as1* cells were incubated with 1NM-PP1 (Fig. 4 D). Together, these data support the notion that Mps1 phosphorylation of Spc29 increases in G1/S during the time of SPB duplication (Lim et al., 1996).

Liquid chromatography (LC)–tandem mass spectrometry (MS; LC-MS/MS) analysis of Spc29 phosphorylated by recombinant Mps1 in vitro identified residues T18, T159, S187, and T240 of Spc29 as Mps1 phosphorylation sites (Fig. 4 E). In vitro phosphorylation of purified Spc29 mutant proteins with altered phosphorylation sites indicated that T18, S187, and T240 are the major amino acids in Spc29 that are modified by Mps1 (Fig. S2 D). Inactivation of all four phosphorylation sites in Spc29 reduced the level of Mps1 phosphorylation to 9% of that conferred upon wild-type Spc29 (spc29-4A; Fig. S2 D).

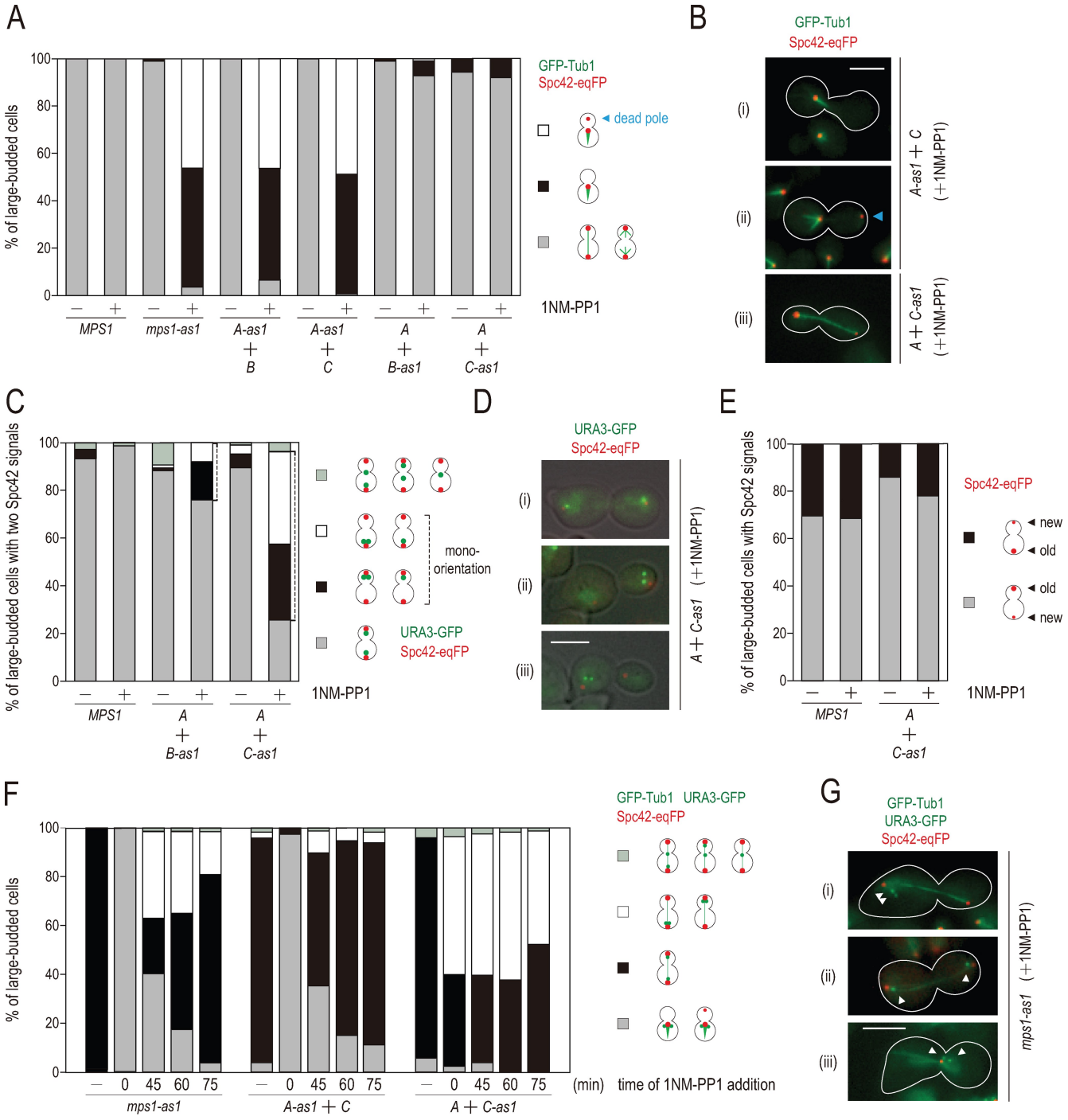

Figure 3. **aa 201–300 of Mps1 function in SPB duplication, and aa 151–200 function in kinetochore biorientation.** (A and B) *GFP-TUB1 SPC42-eqFP* cells with the indicated *MPS1* genotypes were synchronized by α-factor and released with or without 1NM-PP1. After 120 min at 23°C, cells were analyzed for SPB duplication and spindle formation. (A) $n > 100$ large-budded cells were categorized as indicated. (B) Examples of large-budded *mps1-A–as1 mps1-C* cells with only a monopolar spindle (i), a dead pole next to a monopolar spindle (ii; arrowhead), or an anaphase spindle of *mps1-A mps1-C–as1* cells (iii) are shown. (C and D) *MPS1*, *mps1-A mps1-B–as1*, and *mps1-A mps1-C–as1* cells with *SPC42-eqFP URA3-GFP* were cultured as in A. (C) The localization of *URA3*-GFP relative to the pole marker Spc42-eqFP was categorized. (D) Prominent phenotypes of *mps1-A mps1-C–as1* cells are shown. Biorientation of *URA3*-GFP (i), both *URA3*-GFP signals in the bud (ii), and both *URA3*-GFP signals in the mother (iii) are shown. (E) The newly assembled SPB of *mps1-A mps1-C–as1* cells was inherited preferentially to the mother cell even in the presence of 1NM-PP1. Cells of C were categorized as indicated. (F and G) *mps1-A–as1 mps1-C* cells show biorientation of sister kinetochores in the presence of 1NM-PP1. (F) The indicated cell types with *SPC42-eqFP GFP-TUB1* and *URA3*-GFP were arrested by α-factor at 23°C. After 3 h, cells were washed and split into five subcultures. At time 0, 45, 60, and 75 min, 1NM-PP1 was added to four of the cultures to inactivate mps1-as1. No 1NM-PP1 was added to the fifth culture (−). All cells were analyzed 120 min after release for sister kinetochore biorientation. (G) Examples of phenotypes of *mps1-as1* cells (t = 45 min). Both *URA3*-GFP signals in mother cell (i), biorientation of *URA3*-GFP (ii), and monopolar spindle (iii) are shown. Arrowheads indicate *URA3*-GFP signals. (B and G) White lines represent the outline of the yeast cells. Bars, 5 µm.

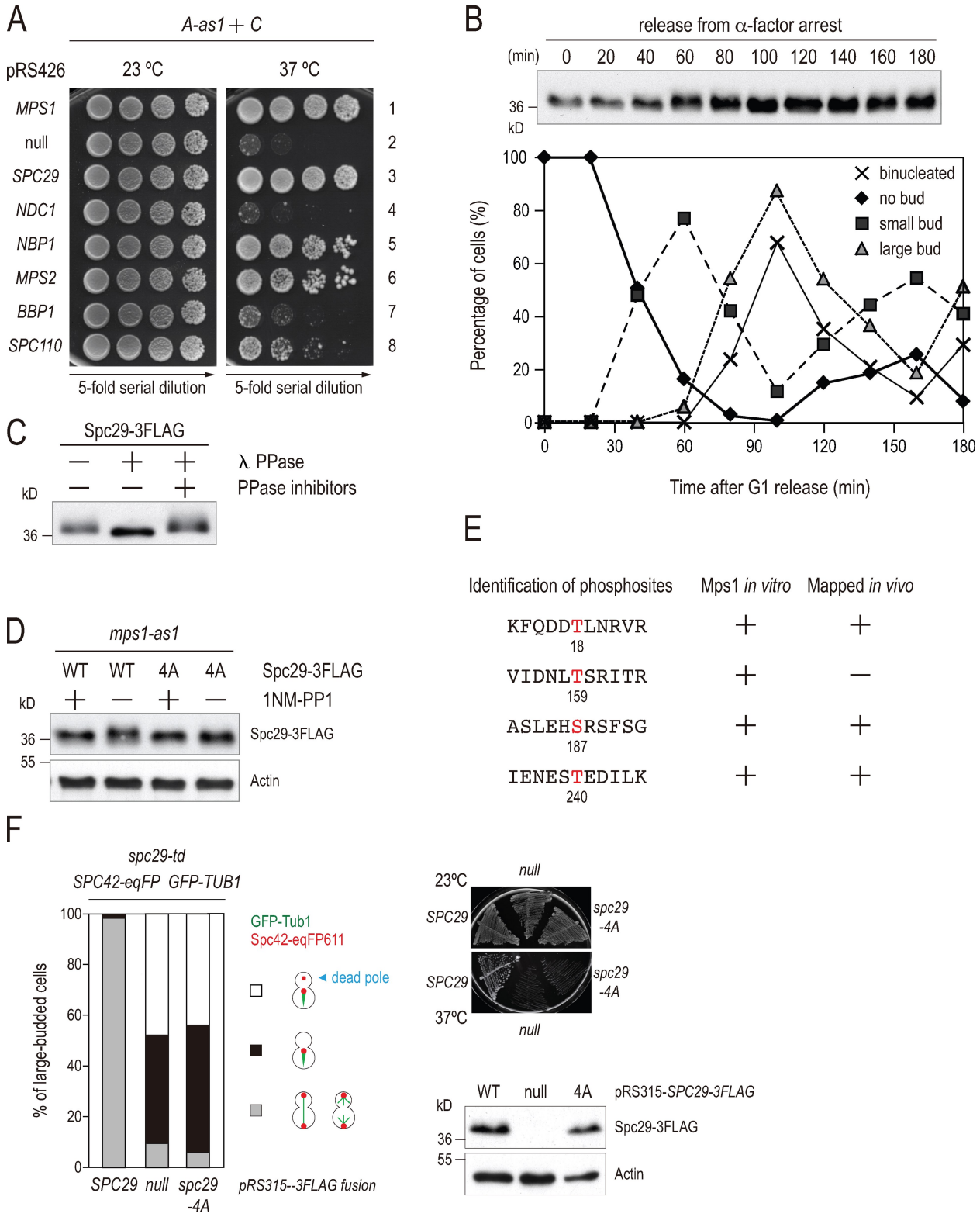

Figure 4. ***SPC29* is a suppressor of the growth defect of *mps1-A–as1 mps1-C* cells.** (A) *mps1-A–as1 mps1-C* cells with 2 μm–based plasmids carrying the indicated wild-type genes were incubated as serial dilutions at 23 and 37°C. (B) Spc29 is phosphorylated in G1/S. *SPC29-3Flag* cells were synchronized in G1 with α-factor and released at 23°C. Immunoblot with anti-Flag antibody is shown. The budding index is shown below. (C) Cells of B were collected after 60 min, and immunoprecipitated Spc29-3Flag was incubated as indicated. Immunoblot with anti-Flag antibody is shown. (D) Spc29 is phosphorylated in an Mps1-dependent manner. *mps1-as1* cells expressing either Spc29-3Flag or spc29-4A–3Flag proteins were grown with or without the addition of 1NM-PP1. An anti-Flag immunoblot is shown. (E) LC-MS/MS analysis identified four Mps1 phosphorylation sites (red) in Spc29: T18, T159, S187, and T240. (F) *spc29-4A* cells have the same phenotype as Spc29-depleted cells. *spc29-td* cells with the indicated plasmids were synchronized in G1 with α-factor at 23°C. Cells were then shifted to 37°C with *UBR1* induction (galactose addition). After 150 min, cells were analyzed for SPB duplication and spindle formation. $n > 100$ large-budded cells per strain type were categorized. The growth of cells on galactose plates and immunoblots (anti-Flag and antiactin antibodies) of extracts of *spc29-td* cells with the indicated plasmids after 150 min of *UBR1* induction at 37°C is also shown. WT, wild type.

In vivo phosphorylation of Spc29 on T18, S187, and T240 was recently reported (Chi et al., 2007; Holinger et al., 2009; Holt et al., 2009). Our LC-MS/MS analysis of purified Spc29-TAP from yeast cells confirmed phosphorylation of T18 and S240 in vivo (Fig. 4 E). The spc29-4A mutant protein, which lacks all four Mps1 phosphorylation sites of Spc29, migrated at the same position on the SDS-PAGE gel as Spc29 from *mps1-as1* cells incubated with 1NM-PP1 (Fig. 4 D). Thus, Spc29 is phosphorylated by Mps1 in vivo.

We next analyzed whether the phosphorylation cycle of Spc29 is important for its function. If dynamic phosphorylation of Spc29 on these residues were to be crucial for it to execute its essential role, we would expect both the phosphorylation-deficient *spc29-4A* and the phosphorylation-mimicking *spc29-4D* mutants to fail to provide *SPC29* function. Indeed, the *spc29-4A* and *-4D* alleles were unable to support the growth of *spc29Δ* cells (Fig. S2 E) despite the fact that both proteins were expressed to similar levels as the wild-type protein (Fig. S2 F). These data and Fig. 4 D suggest that Mps1 has, in our strain background, no major role in stabilizing the Spc29 protein. Analysis of *spc29-4A* in an *SPC29* degron strain (*spc29-td*; Dohmen et al., 1994), which allows efficient degradation of wild-type Spc29 upon shifting cells to 37°C, revealed that *spc29-4A* cells have the same phenotype as Spc29-depleted cells (Fig. 4 F). Thus, the nonphosphorylated spc29-4A does not show any SPB duplication function.

We also analyzed mutations in single phosphorylation sites of Spc29 (Fig. S2 E). *spc29-S187D* supported growth of cells as wild-type *SPC29*, whereas *spc29-S187A* cells were inviable. In contrast, *spc29-T18A*, *-T18D*, *-T240A*, and *-T240D* failed to support the growth of cells despite stable expression of mutant proteins (Fig. S2 F). This suggests that the individual Mps1 phosphorylation sites of Spc29 may have distinct functions. In conclusion, the phosphorylation cycle of Spc29 is important for the viability of cells.

SPB duplication defect of *mps1-A–as1 mps1-C* cells

To understand the molecular role of Mps1 in SPB duplication, we characterized SPB duplication of *mps1-A–as1 mps1-C* cells in greater detail. This experiment was performed with G1/S-arrested cells (*SIC1* overexpression; Schwob et al., 1994) to avoid diffusion of the difficult to detect dead pole away from the preexisting SPB (Araki et al., 2006). Thin serial section electron microscopic analysis of *mps1-A–as1 mps1-C* cells without the inhibitor showed two functional, NE-inserted SPBs that were still connected by the bridge structure (Fig. 5 A). This is the SPB phenotype of cells arrested in G1/S (Byers and Goetsch, 1975). *mps1-A–as1 mps1-C* cells incubated with 1NM-PP1 showed a distorted SPB that had a similar defect to that seen in *spc29-3* cells (Fig. 5, B and C; Elliott et al., 1999). Frequently, an SPB duplication intermediate, which was not inserted in the NE, was associated with the larger, NE-embedded SPB structure (Fig. 5 C).

Mps1 regulates binding of the Mps2–Bbp1 complex to Spc29

To obtain a molecular understanding of Mps1 in SPB duplication, we analyzed the binding of SPB proteins to the dead pole of *mps1-A–as1 mps1-C* cells in the presence of 1NM-PP1. This analysis showed that Spc29, Ndc1, and Nbp1 were associated with the defective SPB, whereas the Mps2–Bbp1 complex and Spc110 were mostly not (Fig. 6, A and B). Similar results were obtained when *mps1-A–as1 mps1-C* cells were shifted to 37°C (Fig. S2 G). The failure of Spc110 to bind to the dead pole is a phenotype exhibited by all SPB insertion mutants because Spc110 only binds to the SPB after the insertion of the duplication plaque into the NE (Kilmartin and Goh, 1996). The absence of the Mps2–Bbp1 complex from the dead pole was unexpected and may indicate that Mps1 facilitates the recruitment of the Mps2–Bbp1 complex to the new SPB.

Previously, we have shown that Bbp1 interacts with Spc29 (Schramm et al., 2000). To confirm a role for Mps1 in the regulation of the interaction between Spc29 and Bbp1, we asked whether the *spc29-4D* allele was able to recruit Bbp1 to the newly formed SPB of *mps1-A–as1 mps1-C* cells incubated at 37°C. High gene dosage of *SPC29* or *spc29-4D* was partly able to recruit Bbp1 to the dead pole (Fig. 6 C), although they were not able to suppress the growth defect of *mps1-A–as1 mps1-C* cells (not depicted). In this assay, *spc29-4D* was clearly more efficient than *SPC29* in bringing Bbp1 to the dead pole, suggesting that the phosphorylation-mimicking *spc29-4D* allele is able to bypass the requirement for Mps1 in the recruitment of Bbp1 to the SPB during the duplication process. In contrast, *spc29-4A* did not significantly increase binding of Bbp1-GFP to the newly formed SPB of *mps1-A–as1 mps1-C* cells. These data suggest that phosphorylation of Spc29 by Mps1 facilitates recruitment of the Mps2–Bbp1 complex to the newly formed SPB.

In vitro experiments tested whether Mps1 regulates the binding of Spc29 to Bbp1. We incubated purified GST-Spc29 with either 6His-Mps1WT or the kinase-dead 6His-msp1KD in the presence of ATP, after which the kinase molecules were efficiently removed from the SPB component by the addition of Ni–nitrilotriacetic acid beads (Fig. 6 D, bottom). Phosphorylated GST-Spc29 showed a moderate gel shift compared with nonphosphorylated GST-Spc29 (Fig. 6 D, top; compare lane 2 with lane 3). In the next step, equal quantities of GST-Spc29 (Fig. 6 D, lanes 2 and 3) and GST (lane 1) were incubated with Bbp1-TAP (lanes 4, 6, and 8) or TAP (lanes 5 and 7). The levels of GST-Spc29 (Fig. 6 D, lanes 5–8) and GST (lane 4) bound to the Bbp1-TAP or TAP beads were determined by quantitative immunoblotting. Neither GST nor GST-Spc29 bound to Bbp1-TAP (Fig. 6 D, lane 4) or TAP beads, respectively (lanes 5 and 7). Importantly, phosphorylation of Spc29 by Mps1 enhanced binding of Spc29 to Bbp1 fivefold (Fig. 6, D [compare lane 6 with lane 8] and E). Thus, binding of Spc29 to Bbp1 is stimulated by Mps1 kinase activity.

Mps1 phosphorylates the yeast centrin Cdc31

Analysis of *mps1-as1* cells revealed distinct SPB phenotypes depending on when in the cell cycle the inhibitor 1NM-PP1 was added. The addition of 1NM-PP1 to synchronized G1-phase cells (α-factor release; satellite is already formed; Byers and Goetsch, 1975) caused SPB duplication defects that were associated with the occurrence of a dead pole (Fig. 3 A).

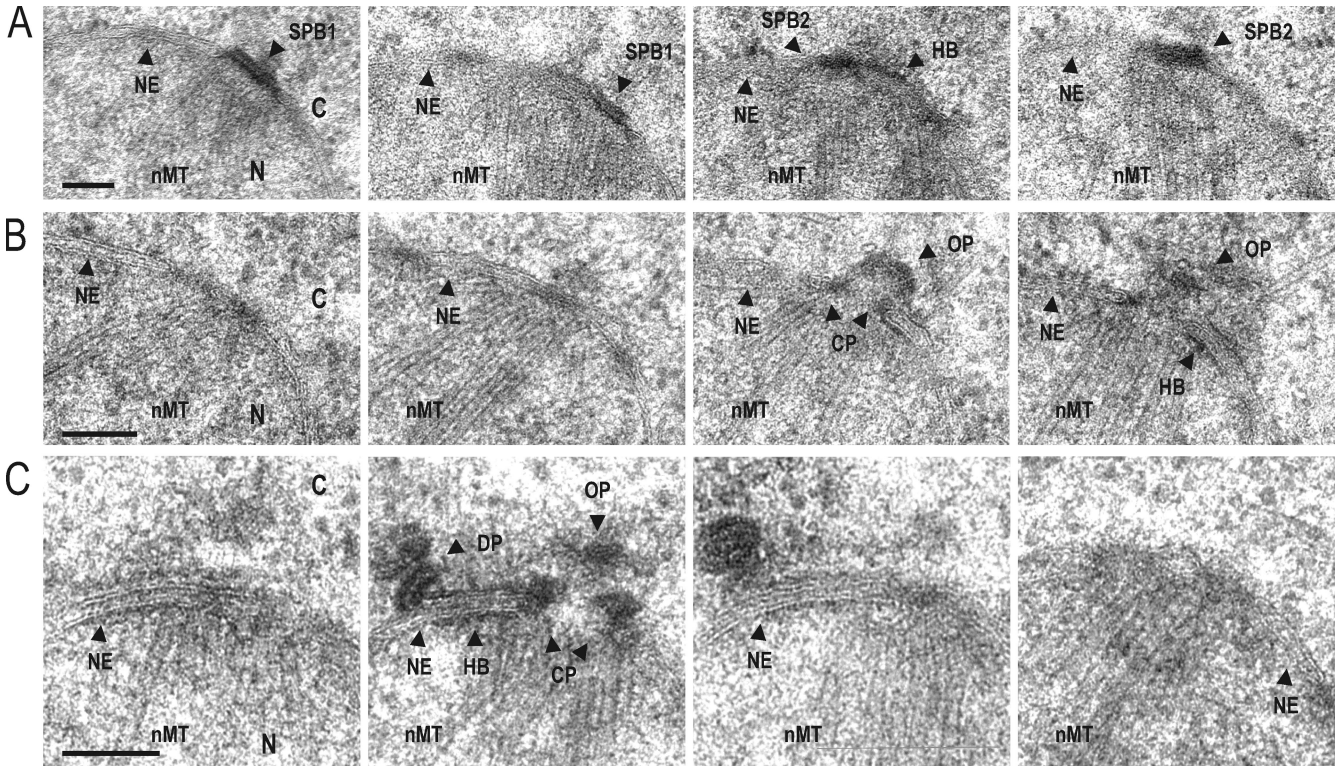

Figure 5. **SPB duplication defect of *mps1-A–as1 mps1-C* cells.** (A–C) Four consecutive serial sections of *mps1-A–as1 mps1-C* cells. α-factor–synchronized *mps1-A–as1 mps1-C* cells carrying a Gal1-*SIC1* overexpression construct were released into galactose medium with (B and C) and without 1NM-PP1 (A). Overexpression of *SIC1* stopped cell cycle progression in G1/S. Thin serial sections of freeze-substituted cells were analyzed by EM. C, cytoplasm; CP, central plaque; DP, duplication plaque; HB, half bridge; N, nucleus; nMT, nuclear MT; OP, outer plaque. Bars, 100 nm.

This phenotype is consistent with the function of Mps1 in the insertion of the duplication plaque into the NE (Schutz and Winey, 1998). However, when 1NM-PP1 was added to synchronized *mps1-as1* cells in S/M phase (cells have already duplicated the SPB), nearly 100% of cells formed a proper anaphase spindle (Fig. 7 A, 120 min) and then exited mitosis into the second cell cycle. In the second cell cycle, the SPB failed to duplicate, as indicated by a single Spc42-eqFP SPB signal; however, a dead pole was rarely observed (Fig. 7 A, 240 min). This suggests that cells progressing from mitosis in G1 without Mps1 activity fail SPB duplication before duplication plaque formation probably on the level of satellite assembly (Schutz and Winey, 1998).

In contrast to *mps1-as1* cells, when 1NM-PP1 was added to *mps1-A–as1 mps1-C* cells in S/M phase, a dead pole was observed in the second cell cycle in at least 30% of cells (Fig. 7 A). Thus, *mps1-A–as1 mps1-C* cells are specifically defective in duplication plaque insertion and not in the initial events of SPB duplication. The multiple defects of *mps1-as1* cells in SPB duplication suggest that there are further Mps1 targets in addition to Spc29.

Purification of a stabilized Mps1 in a proteasome mutant was used to identify additional Mps1 substrates. LC-MS/MS analysis of the proteins in complex with Mps1-TAP revealed components of the Ndc80 complex, the kinetochore proteins Spc105 and Mtw1 (Westermann et al., 2007), and the yeast centrin Cdc31 (Fig. 7 B), which functions early in SPB duplication in the formation of the satellite (Baum et al., 1986).

Cdc31 is an in vitro substrate of Mps1 (Fig. S3 A, second lane). LC-MS/MS analysis of in vitro phosphorylated Cdc31 identified Mps1 phosphorylation sites in Cdc31 at T110 and T128 (Fig. 7 C and Fig. S3 B). T110 is the major phosphorylation site because mutation to alanine radically reduced the ability of Mps1 to phosphorylate Cdc31 in vitro (Fig. S3 A). LC-MS/MS analysis of the functional Z-tagged Cdc31 purified from yeast cells (Kilmartin, 2003) confirmed phosphorylation of T110 in vivo (Fig. S3 C).

To understand the relevance of the Cdc31 phosphorylation, we assessed the phenotypes of *cdc31-T110* and *-T128* phosphorylation mutants. *cdc31-T110A*, *-T110D*, *-T128A*, and *-T128D* supported the essential function of *CDC31* (Figs. S3 D). However, *cdc31-T110A* cells were sensitive for growth at evaluated temperatures (Fig. 7 D). In fact, *cdc31-T110A* cells failed to duplicate their SPB at 37°C, as indicated by the arrest as large-budded cells with a single SPB and a monopolar spindle (Fig. 7 E). As expected from the early function of Cdc31 in SPB duplication (Baum et al., 1986), no dead pole was observed in *cdc31-T110A* cells. These data suggest that the Mps1 phosphorylation cycle on T110 of Cdc31 is important for SPB duplication.

To understand the nature of the defect conferred by blocking T110 phosphorylation, we tested genes coding for SPB components for their ability to suppress the growth defect *cdc31-T110A* cells at 33/35°C. *KAR1* on a CEN-based plasmid was able to confer partial suppression of the growth defect of *cdc31-T110A* cells (Fig. 7 F). Note that high gene dosage of *KAR1* is lethal for cells (Rose and Fink, 1987). Other genes involved in SPB duplication (e.g., *BBP1*, *NBP1*, *SPC29*, *SFI1*,

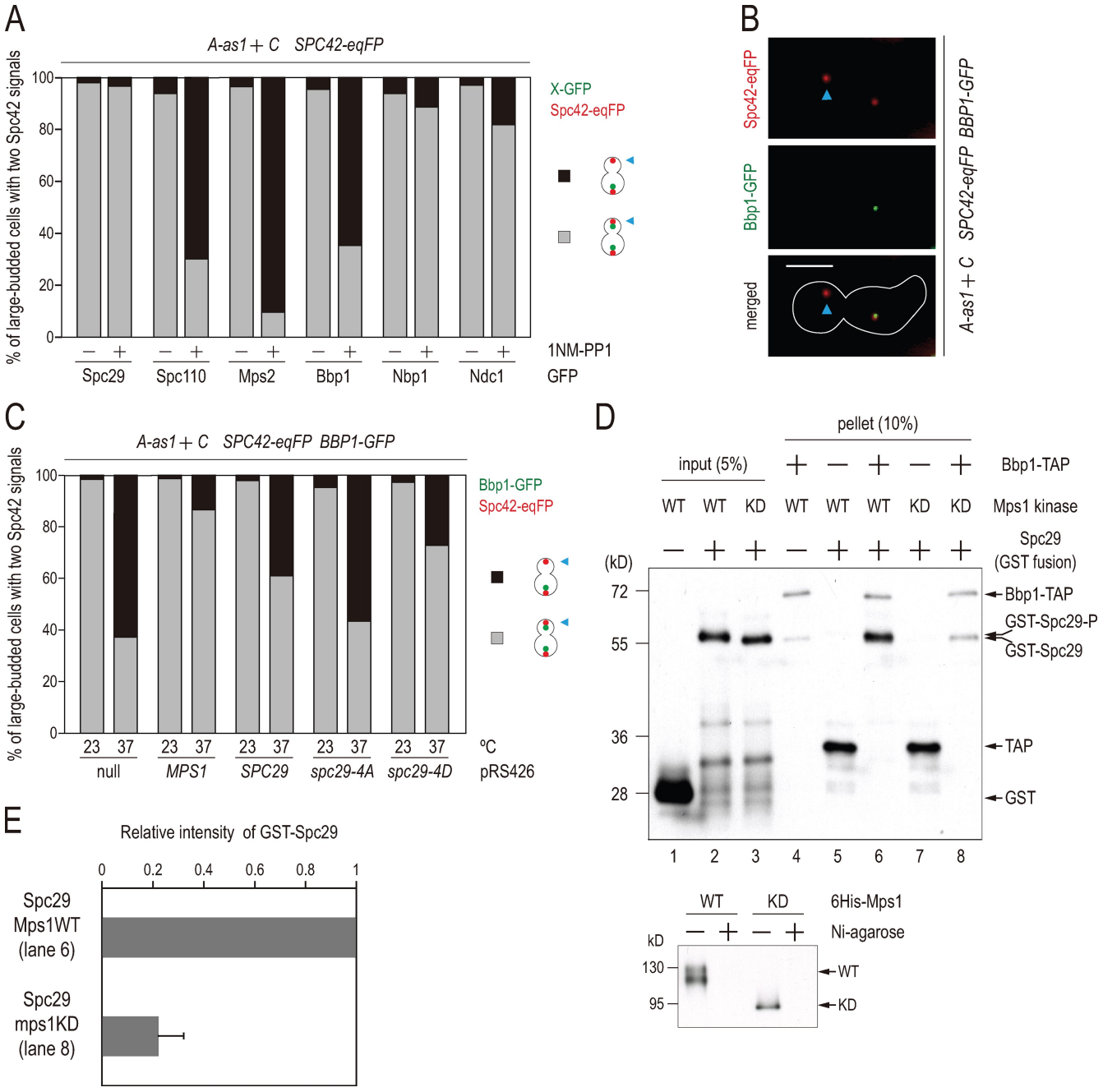

Figure 6. **Mps1 regulates binding of the Mps2–Bbp1 complex to Spc29.** (A and B) Mps2 and Bbp1 are not associated with the dead pole of *mps1-A–as1 mps1-C* cells. (A) *mps1-A–as1 mps1-C* cells with the indicated GFP constructs and *SPC42-eqFP* were synchronized by α-factor and released with DMSO (−) or with 1NM-PP1. Large-budded cells with two Spc42-eqFP signals were analyzed for the colocalization of the second GFP-tagged SPB component. $n > 100$ large-budded cells per cell type. (B) Example of *mps1-A–as1 mps1-C SPC42-eqFP BBP1-GFP* cell from A without Bbp1-GFP at dead pole. The white line represents the outline of the yeast cells. (C) The phosphorylation-mimicking *spc29-4D* is able to bypass the requirement of Mps1 to recruit Bbp1 to the newly developed SPB. *mps1-A–as1 mps1-C* cells with *SPC42-eqFP BBP1-GFP* were grown for 2 h at 37°C in the presence of plasmid-encoded *SPC29*, *spc29-4A*, or *spc29-4D*. Large-budded cells with two Spc42-eqFP signals were analyzed for colocalization of the Bbp1-GFP signal. $n > 100$ large-budded cells per cell type. (A–C) Blue arrowheads mark the dead pole. (D) Mps1 regulates the binding of Spc29 to Bbp1. Recombinant GST (lane 1) and GST-Spc29 (lanes 2 and 3) were incubated with 6His-tagged Mps1 or 6His-mps1KD in the presence of ATP for 1.5 h. 6His-Mps1 proteins were efficiently removed with Ni–nitrilotriacetic acid beads (bottom). GST (lane 4) or GST-Spc29 (lanes 5–8) was then incubated with TAP (lanes 5 and 7) or TAP-tagged Bbp1 (lanes 4, 6, and 8) purified from yeast cells. After washing, the binding reaction was analyzed by immunoblotting with the indicated antibodies. WT, wild type; KD, kinase dead. (E) Relative binding efficiency was determined as described in Materials and methods. Error bars indicate SD. Bar, 5 µm.

and *MPS3*) were unable to suppress the *cdc31-T110* growth defect even when present in high gene dosage (unpublished data). Thus, T110 of Cdc31 is important for the functional interaction with the Kar1 protein.

Mps1 regulates the binding of Cdc31 to Kar1

As T110 is the major Mps1 phosphorylation site in Cdc31 (Fig. S3 A), it may be important for the association of Cdc31

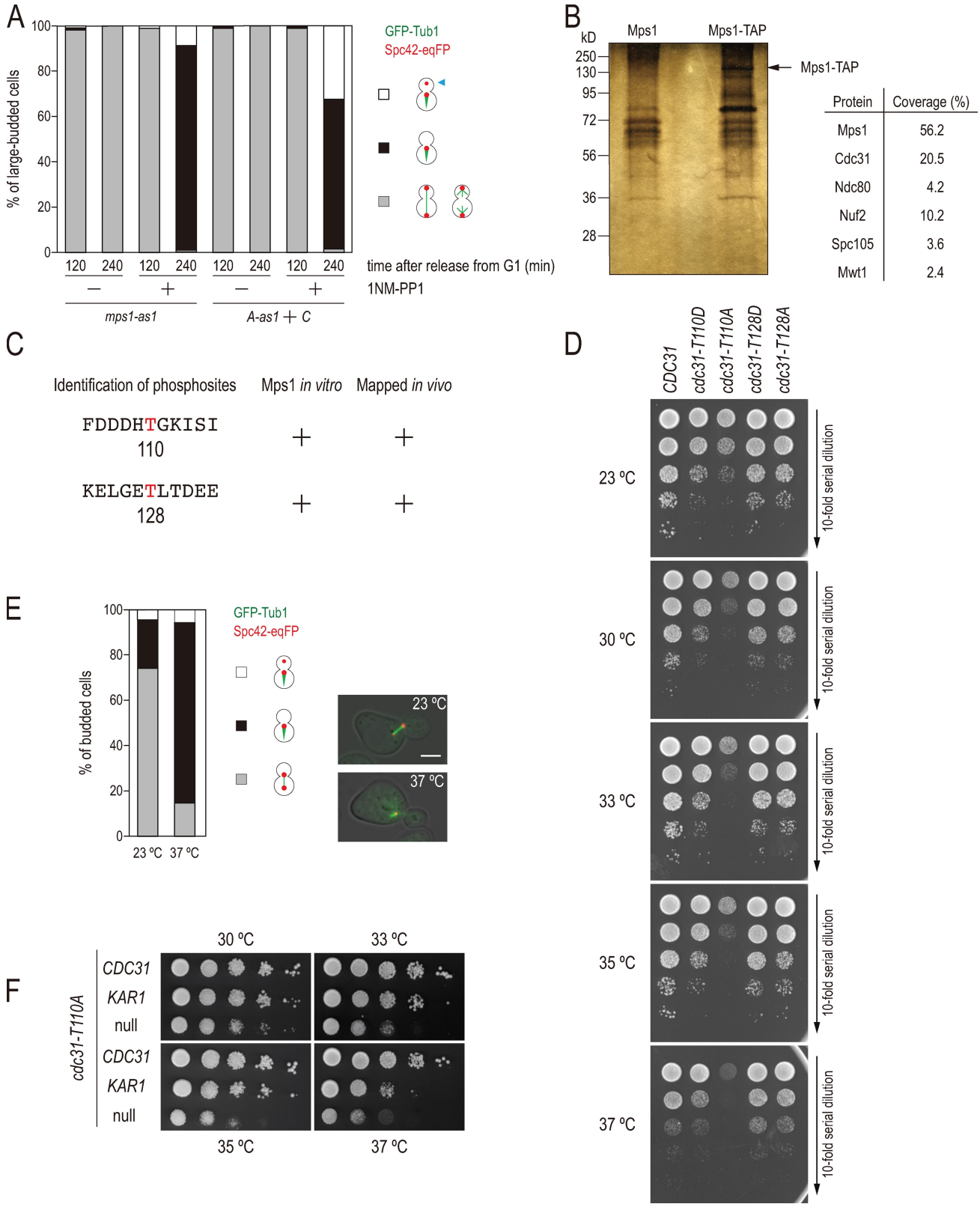

Figure 7. **Mps1 phosphorylates Cdc31.** (A) Mps1 is required early in G1 for SPB duplication. *GFP-TUB1 SPC42-eqFP* cells with the indicated *MPS1* genotypes were synchronized with α-factor at 23°C (t = 0). 1NM-PP1 was added at 75 min when most of the cells had short spindles. Samples were analyzed for SPB duplication and spindle formation at 120 and 240 min. *n* > 100 large-budded cells per condition were categorized. The blue arrowhead marks the dead pole. (B) TAP tag purification of Mps1-TAP from *cim3* cells incubated at 37°C for 2 h. Subsequent LC-MS/MS analysis identified Cdc31 and kinetochore components. (C) T110 and T128 are phosphorylated in vitro and in vivo. LC-MS/MS analysis identified two Mps1 phosphorylation sites (red) in Cdc31. (D) *cdc31-T110A* cells are temperature sensitive for growth. Serial dilutions of the indicated *cdc31* alleles were grown at different temperatures. (E) *cdc31-T110A* cells fail to duplicate the SPB. *cdc31-T110A* cells with *SPC42-eqFP GFP-TUB1* were shifted to 37°C for 2 h and analyzed as illustrated. (F) *cdc31-T110A* cells with CEN plasmids encoded *CDC31* or *KAR1* or the empty plasmid were tested for growth as indicated. Bar, 5 μm.

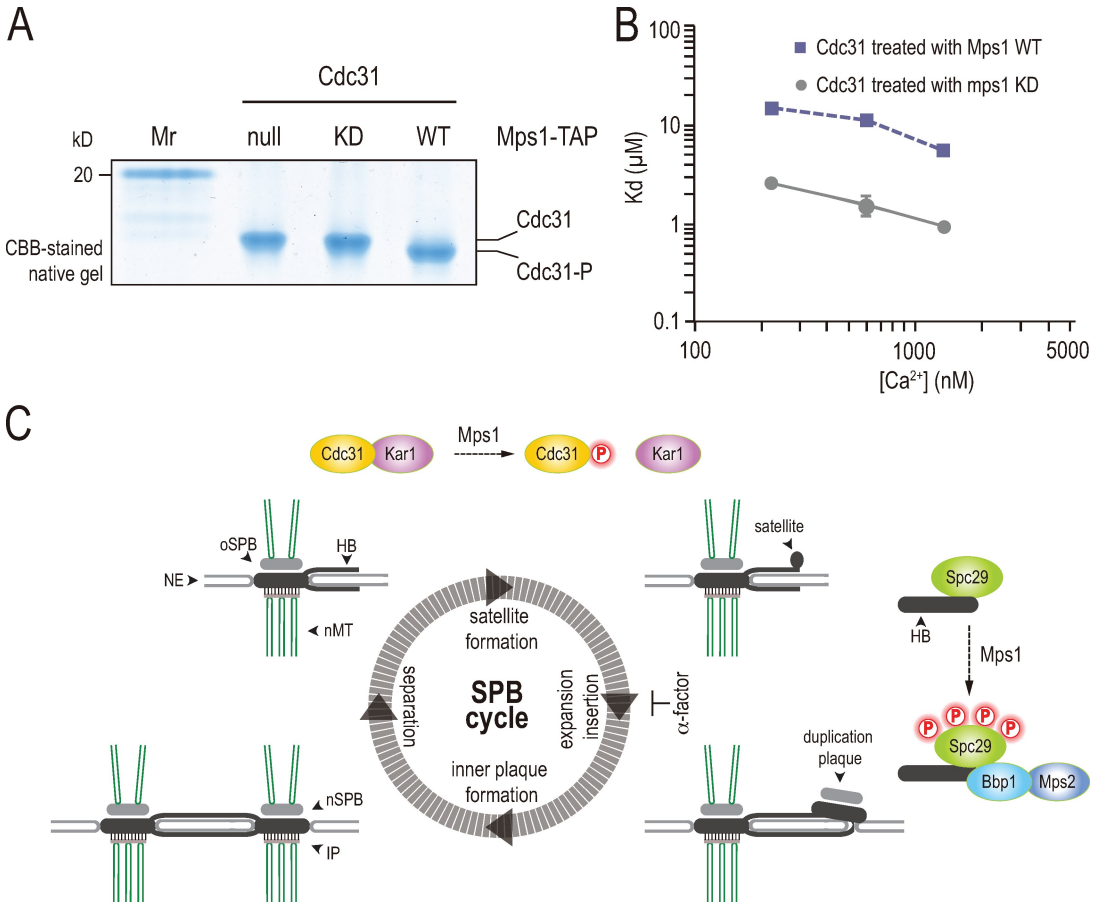

Figure 8. **Mps1 regulates binding of Cdc31 to Kar1.** (A) In vitro kinase reaction using Cdc31 as a substrate for Mps1WT and mps1KD. A CBB-stained 15% native gel of Cdc31 is shown. (B) Ca^{2+}-dependent binding of phosphorylated (Mps1WT; squares) and nonphosphorylated (mps1KD; circles) Cdc31 to the 19-residue Kar1 peptide. Dissociation constants (K_d) were determined using changes in the tryptophan fluorescence spectrum of the peptide upon the addition of Cdc31. Error bars indicate SD. (C) Model for the function of Mps1 at SPBs. See Discussion for details. HB, half bridge; IP, inner plaque; KD, kinase dead; Mr, molecular mass marker; nMT, nuclear MT; nSPB, new SPB; oSPB, old SPB; WT, wild type.

with the SPB component Kar1 (Fig. 7 F). We addressed this directly by comparing the ability of nonphosphorylated Cdc31 and in vitro phosphorylated Cdc31 (Fig. 8 A) to bind a peptide that constitutes the Cdc31-binding site in Kar1 (Geier et al., 1996). The affinity of phosphorylated Cdc31 toward Kar1 peptide was fivefold lower than the ability of nonphosphorylated Cdc31 (Fig. 8 B). Consistently, the ability of Cdc31-T110D to bind the Kar1 peptide was ∼10-fold lower than that of wild-type Cdc31 (unpublished data).

Discussion

Mps1 is a conserved protein kinase that functions from yeast to human cells in centrosome/SPB duplication, kinetochore biorientation, and the SAC (Winey et al., 1991; Hardwick et al., 1996; Fisk and Winey, 2001; Espeut et al., 2008; Jelluma et al., 2008; Tighe et al., 2008). In this study, we have used a novel combination of deletion analysis and chemical genetics to dissect the role of the noncatalytic regions of Mps1 kinase. We found that distinct regions within the noncatalytic N-terminal domain of Mps1 have specific functions either in SPB duplication or kinetochore biorientation. Our defined N-terminal deletion mutants differ from previously characterized *mps1(ts)* conditional-lethal alleles, which either carried single amino acid substitutions in the kinase domain (e.g., *mps1–737*) or 10 aa substitutions dispersed along the entire N-terminal nonkinase domain (*mps1–8*; Schutz and Winey, 1998; Castillo et al., 2002).

The most interesting deletion alleles were *mps1-A*, *-B*, and *-C* (Fig. 1 A). They did not support growth of yeast cells despite having specific kinase activity that was similar to wild-type Mps1. However, combinations of *mps1-A mps1-B* and *mps1-A mps1-C* restored viability, whereas cells with two copies of either mutant could not. These data suggest intragenic complementation of essential functions by the combined *mps1-A mps1-B* or *mps1-A mps1-C* alleles. To confirm this notion, we inactivated one of the two alleles through the as1 mutation, which allows specific inhibition of the kinase by the addition of the ATP analogue 1NM-PP1 (Bishop et al., 2000). *mps1-A–as1 mps1-C* and *mps1-A mps1-C–as1* cells showed strikingly different phenotypes. The addition of 1NM-PP1 to *mps1-A–as1 mps1-C* cells caused lethality with defects in SPB duplication, although kinetochore biorientation was not affected. In contrast, *mps1-A mps1-C–as1* cells duplicated their SPB as wild-type cells but then had defects in kinetochore biorientation.

In the presence of the inhibitor 1NM-PP1, a large percentage of *mps1-as1* cells show monoorientation of sister kinetochores.

In these *mps1-as1* cells, sister kinetochores bind preferentially to the old spindle pole that moves into the daughter cell (Maure et al., 2007). In contrast, in *mps1-A mps1-C–as1* cells, we did not observe preferential binding of sister kinetochores to one of the two SPBs. This was not because of a defect in SPB inheritance (Pereira et al., 2001). The reason for this difference is unclear, but it is possible that Mps1 has multiple functions during kinetochore biorientation and that only one is disrupted in *mps1-A mps1-C–as1* cells. Similar data were obtained for *mps1-A–as1 mps1-B* and *mps1-A mps1-B–as1* cells. Thus, aa 151–200 of Mps1 are important for kinetochore biorientation but not for SPB duplication. In contrast, aa 201–300 of Mps1 are specifically important for SPB duplication but not biorientation of kinetochores. Our findings emphasize the importance of the N-terminal domain of Mps1 for functional selectivity.

We identified *SPC29*, *NBP1*, and *MPS2* as efficient high dosage suppressors of the lethality of *mps1-A–as1 mps1-C* cells. The growth defect of the pleiotropic *mps1-as1* cells or the kinetochore-defective *mps1-A mps1-C–as1* cells were not suppressed by *SPC29*, *NBP1*, and *MPS2*, indicating allele specificity for this suppression. *SPC29* encodes an essential component of the SPB that functions together with the Mps2–Bbp1–Nbp1 complex in the insertion of the newly formed SPB into the NE. Spc29 interacts via the Bbp1 protein with the integral membrane protein Mps2 (Elliott et al., 1999; Muñoz-Centeno et al., 1999; Schramm et al., 2000).

Several lines of evidences indicate that phosphorylation of Spc29 by Mps1 controls an essential step in SPB duplication and is not just important for Spc29 stabilization (Holinger et al., 2009). First, *spc29-4D* or *-4A* was expressed similarly as *SPC29* in yeast cells, and inhibition of mps1-as1 in our strain background did not decrease the levels of Spc29 (Fig. 4 D and Fig. S2 F). Second, conditional-lethal *spc29-3* cells have a similar SPB duplication defect to that found in *mps1-A–as1 mps1-C* cells (Elliott et al., 1999). Third, Mps1 phosphorylates Spc29 in G1/S when the newly formed SPB becomes inserted into the NE. Fourth, the newly formed SPB of *mps1-A–as1 mps1-C* cells that is not inserted into the NE contains Spc29, Nbp1, and the integral membrane protein Ndc1 but is devoid of the Bbp1–Mps2 complex. This may indicate that phosphorylation of Spc29 by Mps1 on four sites recruits the Bbp1–Mps2 complex to the newly formed SPB to facilitate its insertion into the NE. Fifth, expression of the phosphorylation-mimicking *spc29-4D* in *mps1-A–as1 mps1-C* cells restored the recruitment of Bbp1 to the newly formed SPB. Finally, in vitro experiments with purified GST-Spc29 and Bbp1-TAP showed that the interaction between these proteins relied on the phosphorylation of Spc29 by Mps1 (Fig. 6 D).

Thus, what is the specific function of aa 201–300 of Mps1 in SPB duplication? Purified mps1-C still bound to Spc29 (Fig. S4 A), and its specific kinase activity toward Spc29 was as wild-type Mps1 or mps1-A (Fig. S4 B). It is challenging to determine the subcellular localization of Mps1 proteins because of low expression and the close vicinity of the SPB to clustered kinetochores (Jin et al., 2000). This makes it difficult to exclude that mps1-C is no longer associated with SPBs. However, considering that the function of Cdc31 in SPB duplication and proteins in kinetochore biorientation is maintained in *mps1-C* cells, we suggest that aa 201–300 of Mps1 are specifically required to regulate Spc29 in the context of the SPB.

Mps1 has multiple functions in SPB duplication. The phenotype of the *mps1–8* allele suggests that Mps1 is also important early in SPB duplication (Castillo et al., 2002) along with the half bridge proteins Cdc31, Mps3, Kar1, and Sfi1 (Rose and Fink, 1987; Spang et al., 1993, 1995; Biggins and Rose, 1994; Adams and Kilmartin, 1999; Jaspersen et al., 2002; Kilmartin, 2003). Consistently, the addition of 1NM-PP1 to *mps1-as1* cells in metaphase leads to an SPB duplication defect that is distinct from that seen when the inhibitor is added in late G1 (Fig. 7 A). Purification of Mps1 from yeast cells identified yeast centrin Cdc31 as an interactor of Mps1. Mps1 phosphorylates Cdc31 at T128 and the conserved T110 residue in the third EF hand. Blocking phosphorylation of the major Cdc31 phosphorylation site of Mps1 by mutating it to alanine (*cdc31-T110A*) caused a conditional-lethal growth defect in SPB duplication that was suppressed by a single additional gene copy of *KAR1*. Kar1 is an essential half bridge component that interacts with Cdc31 (Biggins and Rose, 1994; Vallen et al., 1994; Spang et al., 1995; Geier et al., 1996). Our results are consistent with a previous study (Ivanovska and Rose, 2001), in which the *cdc31-57*, which has a T110I exchange, displayed synthetic lethality with the *kar1-Δ17* allele.

Phosphorylation of Cdc31 by Mps1 caused a fivefold decrease in the affinity of Cdc31 for a peptide consisting of the Cdc31 docking site on Kar1. Thus, phosphorylation of Cdc31 by Mps1 may regulate the cell cycle–specific physical association of Cdc31 with Kar1. It will be interesting to see whether mammalian Mps1 regulates centrin-2 through phosphorylation and how this impacts upon centrosome duplication (Fisk and Winey, 2001; Salisbury et al., 2002).

Duplication of the mammalian centrioles and the yeast SPB can be envisioned as self-duplication events that are controlled at different steps alongside the duplication process (Fig. 8 C). One of the first steps in SPB duplication is the formation of the satellite in early G1 phase before the start of the cell cycle. Satellite formation requires the activities of Mps1 kinase and, in addition, the half bridge components Cdc31, Kar1, Mps3, and Sfi1. Our data now suggest that the regulation of the Cdc31–Kar1 interaction by Mps1 is critical in satellite formation. Whether phosphorylation of Cdc31 by Mps1 also regulates the interaction with the half bridge components Sfi1 and Mps3 needs to be investigated (Jaspersen et al., 2002; Kilmartin, 2003; Li et al., 2006).

Phosphorylation of the satellite component Spc42 by Cdk1 after the start of the cell cycle may allow extension of the satellite into a duplication plaque, which is layered on top of the cytoplasmic face of the NE (Donaldson and Kilmartin, 1996; Adams and Kilmartin, 1999; Jaspersen et al., 2004). Spc29 that interacts with Spc42 is already associated with the SPB satellite in early G1 phase of cell cycle, and it probably copolymerizes with Spc42 during satellite extension (Adams and Kilmartin, 1999; Elliott et al., 1999). In this study, we showed that the duplication plaque first associates with a subset of the insertion

machinery: Ndc1, Nbp1, and Spc29. Next, Mps1 kinase phosphorylates Spc29 at several sites, leading to the recruitment of Bbp1 probably in complex with Mps2 (Fig. 8 C). This step triggers the insertion of the SPB into the NE with the concomitant binding of the SPB component Spc110 from within the nucleus (Kilmartin and Goh, 1996; Sundberg et al., 1996; Elliott et al., 1999). When taken together, our data suggest that Mps1 kinase regulates critical steps in SPB duplication through controlling the affinity of structural components of the duplication machinery. We propose a similar function for kinases such as Cdk2, mMps1, and Plk4 in mammalian centrosome duplication (Fisk and Winey, 2001; Bettencourt-Dias and Glover, 2007).

Materials and methods

Yeast strains and growth conditions

Strains are listed in Table S1. Yeast strains were derivatives of YPH499 (Sikorski and Hieter, 1989) unless otherwise indicated. Gene deletions and epitope tagging of genes at their endogenous loci were constructed by PCR-based methods (Janke et al., 2004). Mutations or internal deletions in *MPS1*, *SPC29*, or *CDC31* genes were introduced by the QuikChange site-directed mutagenesis kit (Agilent Technologies). For synchronization, yeast cells were grown in YPDA (yeast extract, peptone, dextrose, and adenine) medium and arrested in G1 by treatment with 10 µg/ml α-factor at 23°C until >95% of cells showed a mating projection. Cells were washed twice with growth medium to remove α-factor. Cells were resuspended in YPDA medium at the indicated temperatures. Synthetic complete medium was used for live cell imaging experiments. 1NM-PP1 was purchased from Merck Biosciences. The *mps1-as1* allele was as described previously (Jones et al., 2005).

Fluorescence microscopy

Cells with chromosomal gene fusions with the fluorophores eqFP611 (Wiedenmann et al., 2002) and GFP (Janke et al., 2004) were analyzed by fluorescence microscopy without fixation. Series of z-focal planes images were collected on a microscope equipped with a 100× NA 1.45 Plan-Fluar oil immersion objective (Carl Zeiss, Inc.), a camera (Cascade; 1K; Photometrics), and MetaMorph software (Universal Imaging Corp.). Images in different z planes were projected and processed in Photoshop (Adobe). No manipulations other than contrast and brightness adjustments were used.

Flow cytometry analysis

The DNA content of 20,000 mid–log phase cells stained with propidium iodide was determined by flow cytometry (FACScan flow cytometer; BD) using CELL QUEST software (BD; Schramm et al., 2000).

EM and sample preparations

Yeast cells processed for EM were high-pressure frozen as described previously (Ding et al., 1993). In brief, cells from mid–log phase cycling culture were harvested by vacuum filtration on 0.45-mm filters (Millipore). The yeast paste was frozen using a high-pressure freezer (HPM-010; ABRA Fluid). Freeze substitution of frozen cells was performed in a freeze substitution device (EM-AFS1; Leica) for 2 d in 0.1% glutaraldehyde, 0.25% uranyl acetate, and 0.01% OsO_4 in acetone at −90°C (Müller-Reichert et al., 2003). The freeze-substituted cells were further embedded in Lowicryl resin (HM20) at −45°C. Thin sections (50–70 nm) were cut by ultramicrotomy, contrasted with 2% uranyl acetate and Reynold's lead citrate, and viewed in an electron microscope (CM120-Biotwin; Philips) operating at 100 kV. Digital acquisitions were made with a charge-coupled device camera (Keen View; Soft Imaging System).

In vitro kinase assays

GST- and 6His-fused Mps1 proteins were expressed in *Escherichia coli* Rosetta (DE3) by adding 0.25 mM IPTG for 3 h at 25°C. The recombinant proteins were eluted either with PreScission Protease (GE Healthcare) for GST-Mps1 or with imidazole for 6His-Mps1. Mps1-TAP proteins were prepared from yeast cells. In brief, *MPS1-TAP* cells were resuspended in lysis buffer (50 mM Tris-Cl, pH 8, 400 mM NaCl, 10% glycerol, 1 mM DTT, 1% Triton X-100, 1 mM PMSF, and complete protease inhibitor cocktail, EDTA free [Roche]) and were lysed with a glass bead homogenizer. The cleared cell extract was then incubated with IgG-Dynabeads (Dynal; Invitrogen) for 1 h at 4°C. After intensive washing steps of the IgG Dynabeads, the bound Mps1 was used for the in vitro phosphorylation experiment. GST-Spc29 and GST recombinant proteins were expressed and purified as described previously (Elliott et al., 1999). Purified GST-tagged recombinant proteins were phosphorylated in vitro by the use of Mps1 kinase purified from *E. coli*. The phosphorylation reactions contained 50 mM Tris-Cl, pH 7.5, 75 mM NaCl, 5% glycerol, 10 mM $MgCl_2$, 1 mM DTT, 10 µM ATP, and 10 µCi γ-[^{32}P]ATP. Reactions were incubated at 30°C for 30 min. Coomassie brilliant blue (CBB)–stained bands were quantified by the Odyssey system (LI-COR Biosciences). ^{32}P-labeled proteins were detected with a PhosphorImager (FLA-300; Fujifilm) and quantified with Image Gauge software (Fujifilm). For the analysis of phosphorylation sites by MS, GST-Spc29 and -Cdc31 were mixed with recombinant Mps1 from *E. coli* as described above in this section but in the presence of 10 mM ATP and incubated at 30°C for 1.5 h. In the experiment in Fig. 1 C, Mps1-TAP and mps1KD-TAP proteins bound to IgG-Dynabeads were incubated at 30°C for 30 min with myelin basic protein (MBP; Invitrogen) as described above in this section.

Phosphatase treatment

Cells were resuspended in lysis buffer (50 mM Tris-Cl, pH 8, 400 mM NaCl, 10% glycerol, 1 mM DTT, 1% Triton X-100, 1 mM PMSF, complete protease inhibitor cocktail, EDTA free, 5 mM EDTA, 50 mM NaF, 2 mM Na_3VO_4, 10 mM $Na_4P_2O_7$, and 60 mM β-glycerophosphate) and were lysed as described in the previous section. Spc29-Flag was immunoprecipitated using anti-Flag antibody M2 (Roche) conjugated to protein G–Dynabeads. Reactions both with and without λ phosphatase (New England Biolabs, Inc.) with and without phosphatase inhibitors (5 mM EDTA, 50 mM NaF, 2 mM Na_3VO_4, 10 mM $Na_4P_2O_7$, and 60 mM β-glycerophosphate) were set up and incubated at 30°C for 30 min. Before removal from the beads, the beads were washed once with lysis buffer. SDS loading buffer was then added to each sample, and these were incubated at 95°C to elute the bound proteins.

MS analysis

Proteins present in the gel lane were visualized with colloidal Coomassie staining. Bands were cut out with a scalpel. Gel slices were reduced, alkylated, and digested with trypsin using a Digest pro MS liquid handling system (Intavis AG). The sample was analyzed by a nano–high-performance LC system (Dionex) coupled to a mass spectrometer (ESI LTQ Orbitrap; Thermo Fisher Scientific). The sample was loaded on a C18 trapping column (Inertsil; LC Packings), and peptides were eluted and separated on an analytical column (75 µm × 150 mm) packed with Inertsil 3-µm C18 material (LC Packings). The column was connected to a nano–electrospray ionization emitter (New Objectives). 1,500 V were applied via liquid junction. One survey scan (resolution, 60,000) was followed by five information-dependent product ion scans in the LTQ. Only doubly and triply charged ions were selected for fragmentation. Tandem mass spectra were extracted by Mascot Distiller and grouped within a precursor m/z tolerance of 0.03 amu and with five intermediate scans at maximum. All MS/MS samples were analyzed using Mascot (Matrix Science). Mascot was set up to search the SwissProt database assuming the digestion enzyme trypsin. Mascot was searched with a fragment ion mass tolerance of 0.20 D and a parent ion tolerance of 4.0 ppm. Scaffold (Proteome Software) was used to validate MS/MS-based peptide identifications. Peptide identifications were accepted if they could be established at >95.0% probability as specified by the Peptide Prophet algorithm (Keller et al., 2002). The peptide sequences of the phosphorylated peptides were additionally confirmed by manual evaluation of the fragment spectra.

In vitro binding of Spc29 to Bbp1

Purified GST-Spc29 proteins were phosphorylated in vitro as described in In vitro kinase assays. In the experiment in Fig. 6 D, purified 6His-Mps1WT wild type or the kinase-dead mutant (6His-mps1KD) was incubated with Ni-agarose to remove 6His-Mps1. The treated proteins were mixed with TAP or Bbp1-TAP–bound beads for 1 h at 4°C. The beads were washed three times with washing buffer (50 mM Tris-Cl, pH 8, 1 mM DTT, 150 mM NaCl, 10% glycerol, and 0.2% Triton X-100). 10% of bound fraction was used for an immunoblot with a GST antibody (GE Healthcare) to detected GST-Spc29. GST proteins were quantified with ImageJ (National Institutes of Health). The efficiency of Spc29 binding to Bbp1 was quantified and calibrated as follows: the intensity of the band in Fig. 6 D (lane 4) was subtracted from GST-Spc29 intensities, and the outcome was divided by the intensities of the Bbp1-TAP and GST-Spc29 inputs. To compare results from multiple experiments, data were normalized to the wild-type Mps1 kinase reaction.

Kar1 peptide binding

Binding of nonphosphorylated and phosphorylated Cdc31 to Kar1 peptide was measured as follows (Geier et al., 1996). Mps1-TAP proteins were prepared from yeast cells with 2 µm–based plasmids carrying *pGal1-MPS1-TAP*. Purified Cdc31 at a concentration of 15 µg/µl was treated with either wild-type Mps1WT-TAP or kinase-dead mps1KD-TAP bound to IgG-Dynabeads for 2 h at 30°C under the same buffer conditions as in the in vitro kinase assay described in In vitro kinase assays. The efficiency of phosphorylation was checked by running 2 µg Cdc31 on a 15% native polyacrylamide gel using the Laemmli buffer system without SDS and staining with SimplyBlue SafeStain (Invitrogen). Fluorescence measurements were performed at 20°C on a spectrofluorometer (FP-6500; Jasco). The wavelength for excitation was 295 nm. Emission spectra were recorded over the range of 300–400 nm. 0.5-µl aliquots of appropriate dilutions of nonphosphorylated or phosphorylated Cdc31 were added to 300 µl of a 1-µM solution of the Kar1 peptide (KKRELIESKWHRLLFHDKK) in Ca^{2+} buffers (Invitrogen) with 225, 602, or 1350 nM free [Ca^{2+}], 30 mM MOPS, and 100 mM KCl, pH 7.3. The emission spectrum of the Kar1 peptide showed a maximum at 350 nm. Binding of Cdc31 resulted in a blue shift of the fluorescence emission maximum to 320 nm accompanied by an increase in fluorescence intensity. Dissociation constants (K_d) were determined by fitting the fluorescence intensity at 320 nm to a single site-specific binding model using the program Prism (GraphPad Software, Inc.). Mean values of three titrations were taken.

Online supplemental material

Fig. S1 shows the function of subdomains of Mps1. Fig. S2 shows growth phenotypes of *mps1-as1* cells and phosphorylation of Spc29 by Mps1. Fig. S3 shows identification of the Mps1 phosphorylation sites in Cdc31 and functionality of *cdc31* phosphorylation mutants. Fig. S4 shows biochemical analyses of Mps1 mutant proteins. Table S1 lists the yeast strains used in this study. Online supplemental material is available at http://www.jcb.org/cgi/content/full/jcb.200910027/DC1.

We thank G. Pereira and I. Hagan for comments on the manuscript, T. Ruppert for the MS analysis, and A. Neuner for the EM. Z-tagged Cdc31 was a gift from J. Kilmartin.

The project was supported by Sonderforschungsbereich 638.

Submitted: 5 October 2009
Accepted: 8 March 2010

References

Adams, I.R., and J.V. Kilmartin. 1999. Localization of core spindle pole body (SPB) components during SPB duplication in *Saccharomyces cerevisiae*. *J. Cell Biol.* 145:809–823. doi:10.1083/jcb.145.4.809

Adams, I.R., and J.V. Kilmartin. 2000. Spindle pole body duplication: a model for centrosome duplication? *Trends Cell Biol.* 10:329–335. doi:10.1016/S0962-8924(00)01798-0

Araki, Y., C.K. Lau, H. Maekawa, S.L. Jaspersen, T.H. Giddings Jr., E. Schiebel, and M. Winey. 2006. The *Saccharomyces cerevisiae* spindle pole body (SPB) component Nbp1p is required for SPB membrane insertion and interacts with the integral membrane proteins Ndc1p and Mps2p. *Mol. Biol. Cell*. 17:1959–1970. doi:10.1091/mbc.E05-07-0668

Baum, P., C. Furlong, and B. Byers. 1986. Yeast gene required for spindle pole body duplication: homology of its product with Ca^{2+}-binding proteins. *Proc. Natl. Acad. Sci. USA*. 83:5512–5516. doi:10.1073/pnas.83.15.5512

Bettencourt-Dias, M., and D.M. Glover. 2007. Centrosome biogenesis and function: centrosomics brings new understanding. *Nat. Rev. Mol. Cell Biol.* 8:451–463. doi:10.1038/nrm2180

Biggins, S., and M.D. Rose. 1994. Direct interaction between yeast spindle pole body components: Kar1p is required for Cdc31p localization to the spindle pole body. *J. Cell Biol.* 125:843–852. doi:10.1083/jcb.125.4.843

Bishop, A.C., J.A. Ubersax, D.T. Petsch, D.P. Matheos, N.S. Gray, J. Blethrow, E. Shimizu, J.Z. Tsien, P.G. Schultz, M.D. Rose, et al. 2000. A chemical switch for inhibitor-sensitive alleles of any protein kinase. *Nature*. 407:395–401. doi:10.1038/35030148

Byers, B., and L. Goetsch. 1975. Behavior of spindles and spindle plaques in the cell cycle and conjugation of *Saccharomyces cerevisiae*. *J. Bacteriol.* 124:511–523.

Castillo, A.R., J.B. Meehl, G. Morgan, A. Schutz-Geschwender, and M. Winey. 2002. The yeast protein kinase Mps1p is required for assembly of the integral spindle pole body component Spc42p. *J. Cell Biol.* 156:453–465. doi:10.1083/jcb.200111025

Chi, A., C. Huttenhower, L.Y. Geer, J.J. Coon, J.E. Syka, D.L. Bai, J. Shabanowitz, D.J. Burke, O.G. Troyanskaya, and D.F. Hunt. 2007. Analysis of phosphorylation sites on proteins from *Saccharomyces cerevisiae* by electron transfer dissociation (ETD) mass spectrometry. *Proc. Natl. Acad. Sci. USA*. 104:2193–2198. doi:10.1073/pnas.0607084104

Ding, R., K.L. McDonald, and J.R. McIntosh. 1993. Three-dimensional reconstruction and analysis of mitotic spindles from the yeast, *Schizosaccharomyces pombe*. *J. Cell Biol.* 120:141–151. doi:10.1083/jcb.120.1.141

Dohmen, R.J., P. Wu, and A. Varshavsky. 1994. Heat-inducible degron: a method for constructing temperature-sensitive mutants. *Science*. 263:1273–1276. doi:10.1126/science.8122109

Donaldson, A.D., and J.V. Kilmartin. 1996. Spc42p: a phosphorylated component of the *S. cerevisiae* spindle pole body (SPD) with an essential function during SPB duplication. *J. Cell Biol.* 132:887–901. doi:10.1083/jcb.132.5.887

Dorer, R.K., S. Zhong, J.A. Tallarico, W.H. Wong, T.J. Mitchison, and A.W. Murray. 2005. A small-molecule inhibitor of Mps1 blocks the spindle-checkpoint response to a lack of tension on mitotic chromosomes. *Curr. Biol.* 15:1070–1076. doi:10.1016/j.cub.2005.05.020

Elliott, S., M. Knop, G. Schlenstedt, and E. Schiebel. 1999. Spc29p is a component of the Spc110p subcomplex and is essential for spindle pole body duplication. *Proc. Natl. Acad. Sci. USA*. 96:6205–6210. doi:10.1073/pnas.96.11.6205

Espeut, J., A. Gaussen, P. Bieling, V. Morin, S. Prieto, D. Fesquet, T. Surrey, and A. Abrieu. 2008. Phosphorylation relieves autoinhibition of the kinetochore motor Cenp-E. *Mol. Cell*. 29:637–643. doi:10.1016/j.molcel.2008.01.004

Fisk, H.A., and M. Winey. 2001. The mouse Mps1p-like kinase regulates centrosome duplication. *Cell*. 106:95–104. doi:10.1016/S0092-8674(01)00411-1

Geier, B.M., H. Wiech, and E. Schiebel. 1996. Binding of centrins and yeast calmodulin to synthetic peptides corresponding to binding sites in the spindle pole body components Kar1p and Spc110p. *J. Biol. Chem.* 271:28366–28374. doi:10.1074/jbc.271.37.22453

Haase, S.B., M. Winey, and S.I. Reed. 2001. Multi-step control of spindle pole body duplication by cyclin-dependent kinase. *Nat. Cell Biol.* 3:38–42. doi:10.1038/35050543

Hardwick, K.G., E. Weiss, F.C. Luca, M. Winey, and A.W. Murray. 1996. Activation of the budding yeast spindle assembly checkpoint without mitotic spindle disruption. *Science*. 273:953–956. doi:10.1126/science.273.5277.953

Holinger, E.P., W.M. Old, T.H. Giddings Jr., C. Wong, J.R. Yates III, and M. Winey. 2009. Budding yeast centrosome duplication requires stabilization of *Spc29* via *Mps1*-mediated phosphorylation. *J. Biol. Chem.* 284:12949–12955. doi:10.1074/jbc.M900088200

Holt, L.J., B.B. Tuch, J. Villén, A.D. Johnson, S.P. Gygi, and D.O. Morgan. 2009. Global analysis of Cdk1 substrate phosphorylation sites provides insights into evolution. *Science*. 325:1682–1686. doi:10.1126/science.1172867

Ivanovska, I., and M.D. Rose. 2001. Fine structure analysis of the yeast centrin, Cdc31p, identifies residues specific for cell morphology and spindle pole body duplication. *Genetics*. 157:503–518.

Janke, C., M.M. Magiera, N. Rathfelder, C. Taxis, S. Reber, H. Maekawa, A. Moreno-Borchart, G. Doenges, E. Schwob, E. Schiebel, and M. Knop. 2004. A versatile toolbox for PCR-based tagging of yeast genes: new fluorescent proteins, more markers and promoter substitution cassettes. *Yeast*. 21:947–962. doi:10.1002/yea.1142

Jaspersen, S.L., and M. Winey. 2004. The budding yeast spindle pole body: structure, duplication, and function. *Annu. Rev. Cell Dev. Biol.* 20:1–28. doi:10.1146/annurev.cellbio.20.022003.114106

Jaspersen, S.L., T.H.J. Giddings Jr., and M. Winey. 2002. Mps3p is a novel component of the yeast spindle pole body that interacts with the yeast centrin homologue Cdc31p. *J. Cell Biol.* 159:945–956. doi:10.1083/jcb.200208169

Jaspersen, S.L., B.J. Huneycutt, T.H.J. Giddings Jr., K.A. Resing, N.G. Ahn, and M. Winey. 2004. Cdc28/Cdk1 regulates spindle pole body duplication through phosphorylation of Spc42 and Mps1. *Dev. Cell*. 7:263–274. doi:10.1016/j.devcel.2004.07.006

Jelluma, N., A.B. Brenkman, N.J. van den Broek, C.W. Cruijsen, M.H. van Osch, S.M. Lens, R.H. Medema, and G.J. Kops. 2008. Mps1 phosphorylates Borealin to control Aurora B activity and chromosome alignment. *Cell*. 132:233–246. doi:10.1016/j.cell.2007.11.046

Jin, Q.-W., J. Fuchs, and J. Loidl. 2000. Centromere clustering is a major determinant of yeast interphase nuclear organization. *J. Cell Sci.* 113:1903–1912.

Jones, M.H., B.J. Huneycutt, C.G. Pearson, C. Zhang, G. Morgan, K. Shokat, K. Bloom, and M. Winey. 2005. Chemical genetics reveals a role for Mps1 kinase in kinetochore attachment during mitosis. *Curr. Biol.* 15:160–165. doi:10.1016/j.cub.2005.01.010

Keller, A., A.I. Nesvizhskii, E. Kolker, and R. Aebersold. 2002. Empirical statistical model to estimate the accuracy of peptide identifications

made by MS/MS and database search. *Anal. Chem.* 74:5383–5392. doi:10.1021/ac025747h

Kemmler, S., M. Stach, M. Knapp, J. Ortiz, J. Pfannstiel, T. Ruppert, and J. Lechner. 2009. Mimicking Ndc80 phosphorylation triggers spindle assembly checkpoint signalling. *EMBO J.* 28:1099–1110. doi:10.1038/emboj.2009.62

Kilmartin, J.V. 2003. Sfi1p has conserved centrin-binding sites and an essential function in budding yeast spindle pole body duplication. *J. Cell Biol.* 162:1211–1221. doi:10.1083/jcb.200307064

Kilmartin, J.V., and P.Y. Goh. 1996. Spc110p: assembly properties and role in the connection of nuclear microtubules to the yeast spindle pole body. *EMBO J.* 15:4592–4602.

Lauzé, E., B. Stoelcker, F.C. Luca, E. Weiss, A.R. Schutz, and M. Winey. 1995. Yeast spindle pole body duplication gene *MPS1* encodes an essential dual specificity protein kinase. *EMBO J.* 14:1655–1663.

Li, S.S.L., A.M. Sandercock, P. Conduit, C.V. Robinson, R.L. Williams, and J.V. Kilmartin. 2006. Structural role of Sfi1p-centrin filaments in budding yeast spindle pole body duplication. *J. Cell Biol.* 173:867–877. doi:10.1083/jcb.200603153

Lim, H.H., P.Y. Goh, and U. Surana. 1996. Spindle pole body separation in *Saccharomyces cerevisiae* requires dephosphorylation of the tyrosine 19 residue of Cdc28. *Mol. Cell. Biol.* 16:6385–6397.

Loog, M., and D.O. Morgan. 2005. Cyclin specificity in the phosphorylation of cyclin-dependent kinase substrates. *Nature*. 434:104–108. doi:10.1038/nature03329

Maure, J.F., E. Kitamura, and T.U. Tanaka. 2007. Mps1 kinase promotes sister-kinetochore bi-orientation by a tension-dependent mechanism. *Curr. Biol.* 17:2175–2182. doi:10.1016/j.cub.2007.11.032

Michaelis, C., R. Ciosk, and K. Nasmyth. 1997. Cohesins: chromosomal proteins that prevent premature separation of sister chromatids. *Cell*. 91:35–45. doi:10.1016/S0092-8674(01)80007-6

Müller-Reichert, T., I. Sassoon, E. O'Toole, M. Romao, A.J. Ashford, A.A. Hyman, and C. Antony. 2003. Analysis of the distribution of the kinetochore protein Ndc10p in *Saccharomyces cerevisiae* using 3-D modeling of mitotic spindles. *Chromosoma*. 111:417–428. doi:10.1007/s00412-002-0220-6

Muñoz-Centeno, M.C., S. McBratney, A. Monterrosa, B. Byers, C. Mann, and M. Winey. 1999. *Saccharomyces cerevisiae MPS2* encodes a membrane protein localized at the spindle pole body and the nuclear envelope. *Mol. Biol. Cell*. 10:2393–2406.

Pereira, G., T.U. Tanaka, K. Nasmyth, and E. Schiebel. 2001. Modes of spindle pole body inheritance and segregation of the Bfa1p-Bub2p checkpoint protein complex. *EMBO J.* 20:6359–6370. doi:10.1093/emboj/20.22.6359

Rose, M.D., and G.R. Fink. 1987. KAR1, a gene required for function of both intranuclear and extranuclear microtubules in yeast. *Cell*. 48:1047–1060. doi:10.1016/0092-8674(87)90712-4

Salisbury, J.L., K.M. Suino, R. Busby, and M. Springett. 2002. Centrin-2 is required for centriole duplication in mammalian cells. *Curr. Biol.* 12:1287–1292. doi:10.1016/S0960-9822(02)01019-9

Schramm, C., S. Elliott, A. Shevchenko, E. Schiebel, and E. Schiebel. 2000. The Bbp1p-Mps2p complex connects the SPB to the nuclear envelope and is essential for SPB duplication. *EMBO J.* 19:421–433. doi:10.1093/emboj/19.3.421

Schutz, A.R., and M. Winey. 1998. New alleles of the yeast MPS1 gene reveal multiple requirements in spindle pole body duplication. *Mol. Biol. Cell*. 9:759–774.

Schwob, E., T. Böhm, M.D. Mendenhall, and K. Nasmyth. 1994. The B-type cyclin kinase inhibitor p40SIC1 controls the G1 to S transition in *S. cerevisiae*. *Cell*. 79:233–244. doi:10.1016/0092-8674(94)90193-7

Shimogawa, M.M., B. Graczyk, M.K. Gardner, S.E. Francis, E.A. White, M. Ess, J.N. Molk, C. Ruse, S. Niessen, J.R. Yates III, et al. 2006. Mps1 phosphorylation of Dam1 couples kinetochores to microtubule plus ends at metaphase. *Curr. Biol.* 16:1489–1501. doi:10.1016/j.cub.2006.06.063

Sikorski, R.S., and P. Hieter. 1989. A system of shuttle vectors and yeast host strains designed for efficient manipulation of DNA in *Saccharomyces cerevisiae*. *Genetics*. 122:19–27.

Spang, A., I. Courtney, U. Fackler, M. Matzner, and E. Schiebel. 1993. The calcium-binding protein cell division cycle 31 of *Saccharomyces cerevisiae* is a component of the half bridge of the spindle pole body. *J. Cell Biol.* 123:405–416. doi:10.1083/jcb.123.2.405

Spang, A., I. Courtney, K. Grein, M. Matzner, and E. Schiebel. 1995. The Cdc31p-binding protein Kar1p is a component of the half bridge of the yeast spindle pole body. *J. Cell Biol.* 128:863–877. doi:10.1083/jcb.128.5.863

Sundberg, H.A., L. Goetsch, B. Byers, and T.N. Davis. 1996. Role of calmodulin and Spc110p interaction in the proper assembly of spindle pole body compenents. *J. Cell Biol.* 133:111–124. doi:10.1083/jcb.133.1.111

Tanaka, T.U., N. Rachidi, C. Janke, G. Pereira, M. Galova, E. Schiebel, M.J. Stark, and K. Nasmyth. 2002. Evidence that the Ipl1-Sli15 (Aurora kinase-INCENP) complex promotes chromosome bi-orientation by altering kinetochore-spindle pole connections. *Cell*. 108:317–329. doi:10.1016/S0092-8674(02)00633-5

Tighe, A., O. Staples, and S. Taylor. 2008. Mps1 kinase activity restrains anaphase during an unperturbed mitosis and targets Mad2 to kinetochores. *J. Cell Biol.* 181:893–901. doi:10.1083/jcb.200712028

Ubersax, J.A., E.L. Woodbury, P.N. Quang, M. Paraz, J.D. Blethrow, K. Shah, K.M. Shokat, and D.O. Morgan. 2003. Targets of the cyclin-dependent kinase Cdk1. *Nature*. 425:859–864. doi:10.1038/nature02062

Vallen, E.A., W. Ho, M. Winey, and M.D. Rose. 1994. Genetic interactions between *CDC31* and *KAR1*, two genes required for duplication of the microtubule organizing center in *Saccharomyces cerevisiae*. *Genetics*. 137:407–422.

Westermann, S., D.G. Drubin, and G. Barnes. 2007. Structures and functions of yeast kinetochore complexes. *Annu. Rev. Biochem.* 76:563–591. doi:10.1146/annurev.biochem.76.052705.160607

Wiedenmann, J., A. Schenk, C. Röcker, A. Girod, K.-D. Spindler, and G.U. Nienhaus. 2002. A far-red fluorescent protein with fast maturation and reduced oligomerization tendency from *Entacmaea quadricolor* (Anthozoa, Actinaria). *Proc. Natl. Acad. Sci. USA*. 99:11646–11651. doi:10.1073/pnas.182157199

Winey, M., L. Goetsch, P. Baum, and B. Byers. 1991. MPS1 and MPS2: novel yeast genes defining distinct steps of spindle pole body duplication. *J. Cell Biol.* 114:745–754. doi:10.1083/jcb.114.4.745

Winey, M., M.A. Hoyt, C. Chan, L. Goetsch, D. Botstein, and B. Byers. 1993. NDC1: a nuclear periphery component required for yeast spindle pole body duplication. *J. Cell Biol.* 122:743–751. doi:10.1083/jcb.122.4.743